



# Whole-genome analyses converge to support the Hemirotifera hypothesis within Syndermata (Gnathifera)

Alexandros Vasilikopoulos · Holger Herlyn · Diego Fontaneto · Christopher Gordon Wilson · Reuben William Nowell · Jean-François Flot · Timothy Giles Barraclough · Karine Van Doninck

Received: 2 March 2023 / Revised: 20 October 2023 / Accepted: 8 December 2023  
© The Author(s), under exclusive licence to Springer Nature Switzerland AG 2024

**Abstract** The clade Syndermata includes the endoparasitic Acanthocephala, the epibiotic Seisonidea, and the free-living Bdelloidea and Monogononta. The phylogeny of Syndermata is highly debated, hindering the understanding of the evolution of morphological features, reproductive modes, and lifestyles within the group. Here, we use publicly available whole-genome

data to re-evaluate syndermatan phylogeny and assess the credibility of alternative hypotheses, using a new combination of phylogenomic methods. We found that the Hemirotifera and Pararotatoria hypotheses were recovered under combinations of datasets and methods with reduced possibility of systematic error in concatenation-based analyses. In contrast, the Seisonidea-sister and Lemniscea hypotheses were recovered under dataset combinations with increased possibility of systematic error. Hemirotifera was further supported by whole-genome microsynteny analyses and species-tree methods that use multi-copy orthogroups after removing distantly related outgroups. Pararotatoria was only partially supported by microsynteny-based phylogenomic reconstructions.

Handling editor: Sidinei M. Thomaz

Guest editors: Maria Špoljar, Diego Fontaneto, Elizabeth J. Walsh & Natalia Kuczyńska-Kippen / Diverse Rotifers in Diverse Ecosystems

**Supplementary Information** The online version contains supplementary material available at <https://doi.org/10.1007/s10750-023-05451-9>.

A. Vasilikopoulos (✉) · K. Van Doninck (✉)  
Research Unit of Molecular Biology and Evolution,  
Université libre de Bruxelles (ULB), 1050 Brussels,  
Belgium  
e-mail: alexvasilikop@gmail.com

K. Van Doninck  
e-mail: Karine.Van.Doninck@ulb.be

H. Herlyn  
Institute of Organismic and Molecular Evolution  
(iomE), Johannes Gutenberg University Mainz,  
55099 Anthropology, Germany

D. Fontaneto  
Molecular Ecology Group (MEG), Water Research  
Institute (IRSA), National Research Council (CNR),  
28922 Verbania Pallanza, Italy

C. G. Wilson · R. W. Nowell · T. G. Barraclough  
Department of Biology, University of Oxford,  
Oxford OX1 3SZ, UK

R. W. Nowell  
Institute of Ecology and Evolution, University  
of Edinburgh, Edinburgh EH9 3FL, UK

J.-F. Flot  
Evolutionary Biology and Ecology, Université libre de  
Bruxelles (ULB), 1050 Brussels, Belgium

J.-F. Flot  
Interuniversity Institute of Bioinformatics in Brussels,  
Université libre de Bruxelles (ULB) - Vrije Universiteit  
Brussel (VUB), 1050 Brussels, Belgium

Hence, Hemirotifera and partially Pararotatoria were supported by independent phylogenetic methods and data-evaluation approaches. These two hypotheses have important implications for the evolution of syndermatan morphological features, such as the gradual reduction of locomotory ciliation from the common ancestor of Syndermata in the stem lineage of Pararotatoria. Our study illustrates the importance of combining various types of evidence to resolve difficult phylogenetic questions.

**Keywords** Phylogenomics · Outgroup selection · Systematic error · Synteny · Rotifera · Acanthocephala

## Introduction

The spiralian clade Syndermata comprises the rotifer clades Bdelloidea, Monogononta, Seisonidea (i.e., the phylum Rotifera sensu stricto, composed of free-living species), and also the phylum Acanthocephala, which contains only species with an endoparasitic lifestyle (Fontaneto & De Smet, 2015; Herlyn, 2021). Species of Acanthocephala and Seisonidea are gonochoristic and reproduce sexually with obligate amphimixis (Ricci et al., 1993; Herlyn, 2021), while species of Monogononta are facultatively sexual and species of Bdelloidea are obligately asexual (Fontaneto & De Smet, 2015; Wallace, 2002; Terwagne et al., 2022). Therefore, the phylogenetic relationships within Syndermata form an ideal system to test hypotheses on the evolutionary transitions among different lifestyles, reproductive modes, and morphological features (Near, 2002; Herlyn et al., 2003; Min & Park, 2009; Fussmann, 2011). A close evolutionary affinity of Acanthocephala to Rotifera is an old hypothesis based on analyses of both morphological and molecular data (von Haffner, 1950; Storch & Welsch, 1969; Ahlrichs, 1995, 1997; Winnepenninckx et al., 1995, 1998; Garey et al., 1996; Wallace et al., 1996). From a morphological perspective, the Syndermata hypothesis is strongly supported by the presence of a syncytial epidermis with an intracytoplasmic lamina (e.g., Storch & Welsch, 1969; Ahlrichs, 1995,

1997; Wallace et al., 1996; Zrzavý, 2001; Wallace, 2002; Sørensen et al., 2016). Molecular studies have also provided substantial evidence in the support of the Syndermata hypothesis (Winnepenninckx et al., 1995; Garey et al., 1996, 1998; García-Varela & Nadler, 2006; Struck et al., 2014; Wey-Fabrizius et al., 2014; Laumer et al., 2015, 2019). However, the evolutionary relationships among syndermatan subgroups are still highly debated (see Fig. 1a–f, e.g., Garey et al., 1996, 1998; Melone et al., 1998; Mark Welch, 2000; Sørensen & Giribet, 2006; García-Varela & Nadler, 2006; Witek et al., 2008; Fontaneto & Jondelius, 2011; Lasek-Nesselquist, 2012; Fontaneto, 2014; Wey-Fabrizius et al., 2014; Fontaneto & De Smet, 2015; Sielaff et al., 2016; Mauer et al., 2021). In the present study, we investigate the phylogeny of Syndermata by leveraging publicly available whole-genome data from all major syndermatan subclades and by using a new combination of phylogenomic approaches.

Early molecular phylogenetic studies of Syndermata showed that Acanthocephala is nested within Rotifera sensu stricto (Garey et al., 1996, 1998; Winnepenninckx et al., 1998; Mark Welch, 2000; Herlyn et al., 2003; García-Varela & Nadler, 2006; Sørensen & Giribet, 2006), a result that was corroborated later by phylogenomic analyses (Witek et al., 2008; Min & Park, 2009; Wey-Fabrizius et al., 2014; Laumer et al., 2015; Sielaff et al., 2016). A clade Acanthocephala+Bdelloidea (i.e., Lemniscea, Fig. 1b, Lorenzen, 1985) was supported by most of these early molecular phylogenetic studies despite the lack of clear morphological synapomorphies (Clément, 1993; Ricci, 1998). On the other hand, a sister group relationship of Bdelloidea and Monogononta (i.e., clade Eurotatoria, Fig. 1c) as well as the monophyly of Rotifera sensu stricto (Fig. 1f), which were traditionally based on morphological and ecological features (Wallace & Colburn, 1989; Melone et al., 1998), gained little support in the molecular era (Witek et al., 2008, 2009; Min & Park, 2009; Lasek-Nesselquist, 2012). Furthermore, the phylogenetic placement of Seisonidea with respect to the other three groups remained unknown at the dawn of the phylogenomics era, due to the lack of genomic data from Seisonidea (e.g., Witek et al., 2008, 2009; Min & Park, 2009; Lasek-Nesselquist, 2012; Hankeln et al., 2014). Despite these observations from molecular studies, according to some researchers, morphological evidence weighs

K. Van Doninck  
Research Unit in Environmental and Evolutionary Biology,  
Université de Namur, 5000 Namur, Belgium

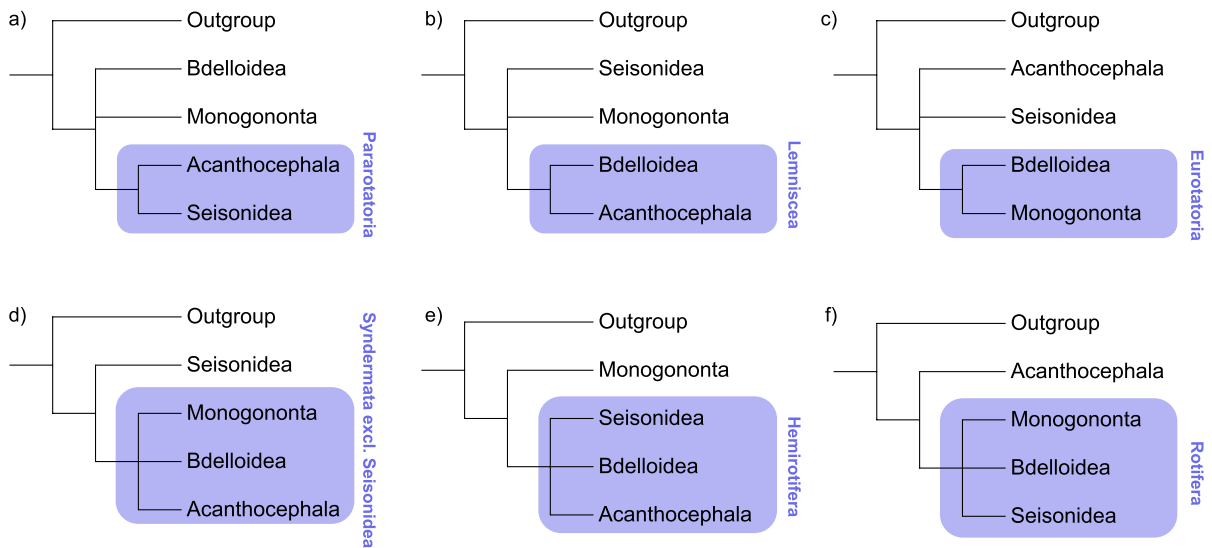


**Fig. 1** Competing hypotheses concerning the phylogenetic relationships of Syndermata based on the results of previous molecular and morphological studies. **a** Seisonidea is the sister group of Acanthocephala (Pararotatoria hypothesis); **b** Acanthocephala is the sister group of Bdelloidea (Lemniscea hypothesis); **c** Bdelloidea and Monogononta are sister groups (Eurotatoria hypothesis); **d** Seisonidea is the sister group of a

clade Acanthocephala + Bdelloidea + Monogononta (i.e., Seisonidea-sister hypothesis); **e** Monogononta is the sister group of a clade Acanthocephala + Bdelloidea + Seisonidea (Hemirotifera or Monogononta-sister hypothesis); **f** Acanthocephala is the sister group of a clade Bdelloidea + Monogononta + Seisonidea (i.e., Rotifera sensu stricto)

against discarding the Eurotatoria and Rotifera hypotheses (Wallace & Colburn, 1989; Melone et al., 1998; Fontaneto & De Smet, 2015).

The absence of typical rotifer characters in species of Acanthocephala is likely due to extreme morphological divergence attributable to their endoparasitic lifestyle (e.g., Mark Welch, 2000, 2005). Additional evidence that acanthocephalans are modified rotifers comes from the early studies of ultrastructural data and sperm morphology (Ahlrichs, 1997, 1998; Ferraguti & Melone, 1999), which suggested that Seisonidea and Acanthocephala are sister groups within the syndermatan clade Pararotatoria (Fig. 1a). Later genomic sampling of Seisonidea in phylogenomic analyses further supported the Pararotatoria hypothesis (Wey-Fabrizius et al., 2014; Sielaff et al., 2016; Mauer et al., 2021). Pararotatoria is considered the sister group of Bdelloidea based on the results of the latest phylogenomic studies of Syndermata (Wey-Fabrizius et al., 2014; Sielaff et al., 2016; Mauer et al., 2021). Consequently, Acanthocephala, Bdelloidea, and Seisonidea are *ipso facto* placed in a monophyletic group (the Hemirotifera hypothesis, see Fig. 1e; Sørensen & Giribet, 2006; Wey-Fabrizius

et al., 2014; Sielaff et al., 2016; Mauer et al., 2021). However, other phylogenomic studies with extensive taxon sampling of Spiralia recovered Seisonidea as sister to all other lineages of Syndermata, suggesting a Seisonidea-sister hypothesis instead of a Monogononta-sister hypothesis (see Fig. 1d; Struck et al., 2014; Laumer et al., 2015). Hence, a reevaluation of the internal phylogeny of Syndermata using new data and methods is needed to test and refine the hypotheses discussed above (Fontaneto, 2014).

Some previous molecular phylogenetic analyses of Syndermata suggested sensitivity of phylogenetic results to the use of distantly related outgroup species, such as flatworm or nematode species (phyla Platyhelminthes and Nematoda, respectively, Herlyn et al., 2003; Lasek-Nesselquist, 2012; Mauer et al., 2021). This phenomenon has also been shown to affect phylogenetic analyses of other taxa (Philippe et al., 2009; Li et al., 2012; Pisani et al., 2015). The phylum Micrognathozoa, consisting of one described species (*Limnognathia maerski*, see Table 1), is the closest known outgroup of Syndermata (Sørensen et al., 2000, 2016; Sørensen, 2002, 2003; Funch et al., 2005; Laumer et al., 2015, 2019; Marlétaz et al.,

**Table 1** Genome and transcriptome datasets analyzed in the present study and their associated statistics. BUSCO gene completeness was assessed using the Metazoa lineage (i.e., 954 genes in total). Percentage of gene completeness is based only on complete BUSCO genes in each proteome; fragmented

genes are not taken into account (see also Online Resource 1: Fig. S1). For the transcriptome of *Limnognathia maerski*, raw reads were downloaded from the NCBI-SRA database (accession: SRR2131287) and processed as described in the text to produce a set of protein sequences

Species	Taxonomic group	Dataset type	Genome assembly accession (GenBank-NCBI)	No. of protein-coding genes*	BUSCO completeness of predicted proteomes (%)	Source of gene annotation	Date of retrieval
<i>Hymenolepis microstoma</i> (Dujardin, 1845)	Platyhelminthes	Genome	GCA_000469805.3	10,139	74.00	WormBase Parasite v. 17.0 (annotation: v. 2018–10-WormBase)	04.07.2022
<i>Schmidtea mediterranea</i> Benazzi, Baguna, Ballester & del Papa, 1975	Platyhelminthes	Genome	GCA_002600895.1	22,045	77.70	PlanMine v. 3.0 (annotation: v. 2 high conf.)	28.09.2022
<i>Limnognathia maerski</i> Kristensen & Funch, 2000	Micrognathozoa	Transcriptome	Not applicable	16,811	70.90	Not applicable	07.07.2022
<i>Seison nebaliae</i> Grube, 1861	Syndermata, Seisonidea	Genome	GCA_023231475.1	11,502	65.00	GenBank-NCBI	28.09.2022
<i>Pomphorhynchus laevis</i> (Zoega in Müller, 1776)	Syndermata, Acanthocephala	Genome	GCA_012934845.2	12,073	54.10	GenBank-NCBI	28.09.2022
<i>Proales similis</i> de Beauchamp, 1907	Syndermata, Monogononta	Genome	GCA_019059635.1	9,469	76.80	Annotated in the present study	03.10.2022
<i>Brachionus calyciflorus</i> Pallas, 1766	Syndermata, Monogononta	Genome	GCA_002922825.1	23,548	90.40	GenBank-NCBI	28.09.2022
<i>Didymodactylos carnosus</i> Milne, 1916	Syndermata, Bdelloidea	Genome	GCA_905250885.1	46,863	82.80	GenBank-NCBI	28.09.2022
<i>Rotaria socialis</i> (Kellicott, 1888)	Syndermata, Bdelloidea	Genome	GCA_905331475.1	32,760	88.90	GenBank-NCBI	28.09.2022
<i>Rotaria sordida</i> (Western, 1893)	Syndermata, Bdelloidea	Genome	GCA_905251635.1	39,313	89.50	GenBank-NCBI	28.09.2022

**Table 1** (continued)

Species	Taxonomic group	Dataset type	Genome assembly accession (GenBank-NCBI)	No. of protein-coding genes*	BUSCO completeness of predicted proteomes (%)	Source of gene annotation	Date of retrieval
<i>Adineta vaga</i> (Davis, 1873)	Syndermata, Bdelloidea	Genome	GCA_021613535.1	31,335	88.50	GenBank-NCBI	28.09.2022
<i>Adineta ricciae</i> Segers & Shiel, 2005	Syndermata, Bdelloidea	Genome	GCA_905250025.1	46,588	88.70	GenBank-NCBI	28.09.2022

\*Note: number of protein-coding genes is given after removing pseudogenes, alternative gene transcripts, or isoforms

2019; Bekkouche & Gąsiorowski, 2022). Bekkouche & Gąsiorowski (2022) suggested the name Gynognathifera for the clade Micrognathozoa + Syndermata. Despite this, no previous phylogenomic study focusing on relationships within Syndermata included data from Micrognathozoa (Wey-Fabrizius et al., 2014; Sielaff et al., 2016; Mauer et al., 2021). More specifically, transcriptomic sampling of Micrognathozoa was only included in a few studies aimed at resolving the phylogenetic position of Micrognathozoa, the phylogeny of Spiralia, or the phylogeny of Metazoa but not specifically the phylogeny of Syndermata (Laumer et al., 2015, 2019; Marlétaz et al., 2019). Since previous phylogenomic studies of Syndermata suggested potential phylogenetic artifacts due to the use of a distantly related outgroup, we re-examined these claims using the more closely related Micrognathozoa as an outgroup.

The phylogeny of Syndermata has also been hypothesized to depend on the taxon sampling of the ingroup, the choice of data for analysis, and the choice of evolutionary model (Melone et al., 1998; Min & Park, 2009; Fontaneto & Jondelius, 2011; Lasek-Nesselquist, 2012; Wey-Fabrizius et al., 2014; Sielaff et al., 2016; Mark Welch, 2000; Mauer et al., 2021). It is now well understood that systematic errors are prevalent in phylogenetic reconstructions based on molecular data across the animal tree of life (Lartillot et al., 2007; Philippe & Roure, 2011; Philippe et al., 2011; Struck et al., 2014). Systematic errors are the result of inadequate evolutionary modeling of the DNA (or amino-acid) substitution process, which is highly heterogeneous (Philippe et al., 2011; Kapli et al., 2020, 2021). The latest molecular

studies of syndermatan relationships suggested potential systematic errors affecting the results of the analyses, but they did not employ site-heterogeneous profile mixture models that account for across-site compositional heterogeneity of the substitution process (Sielaff et al., 2016; Mauer et al., 2021). Other biological processes such as incomplete lineage sorting (ILS) and cross-species gene flow may cause the gene trees to differ from the species tree and can also impede accurate species-tree estimation in concatenation-based analyses (Kubatko & Degnan, 2007; Mendes & Hahn, 2018; Jiao et al., 2020; Kapli et al., 2020; Morel et al., 2022). However, methods that are robust to different biological sources of gene-tree heterogeneity have not yet been applied to infer the phylogeny of Syndermata. Moreover, many of these methods are now optimized to include multi-copy gene families (or orthogroups) for species-tree estimation, therefore drastically increasing the total number of genes for analysis (Smith & Hahn, 2021). This allows us to reexamine the validity of previous phylogenetic results of syndermatan relationships using independent methods that account for different sources of heterogeneity in the data. Additionally, whole-genome data are now available for all syndermatan subgroups, making it possible to investigate the phylogeny of Syndermata using whole-genome structural data (e.g., Drillon et al., 2020; Zhao et al., 2021; Schultz et al., 2023). Such whole-genome structural approaches are less likely to be sensitive to homoplasy and substitution saturation than conventional sequence-based approaches and complement the results of the sequence-based analyses (Niehuis et al., 2012; Lehmann et al., 2013; Sielaff et al., 2016;

Cloutier et al., 2019; Ontano et al., 2021; Zhao et al., 2021; Parey et al., 2023; Schultz et al., 2023). Congruent findings from different methods and datasets should ideally be the aim of modern phylogenomic studies (Tihelka et al., 2021; Vasilikopoulos et al., 2021b). Despite this, the congruence of syndermatan phylogenetic relationships across different analyses has yet to be tested using results from these new genome-scale structural and gene tree-based phylogenomic approaches.

In this study, we re-examine the phylogenetic relationships within Syndermata using a new combination of phylogenomic approaches, namely: 1) concatenation-based analyses using profile mixture models that account for long-branch attraction artifacts due to compositional heterogeneity across sites, 2) species-tree methods that utilize multi-copy orthogroups for phylogenetic inference, and 3) whole-genome microsynteny-based phylogenomic analyses of syndermatan relationships. Our main aim was to test congruence among different methods and datasets concerning some previously suggested phylogenetic relationships of Syndermata (Fig. 1) and to discuss the different approaches while taking into account previous morphological analyses.

## Methods

### Taxon sampling and processing of genomic and transcriptomic datasets

We used 11 published genomes (Syndermata: 9, Platyhelminthes: 2) and one published transcriptome, belonging to the micrognathozoan species *L. maerski*, to address the phylogenetic relationships of Syndermata (Table 1, Online Resource 1: Fig. S1, Laumer et al., 2015; Nowell et al., 2018, 2021; Mauer et al., 2020, 2021; Kim et al., 2021; Simion et al., 2021). Gene annotations were downloaded from the NCBI, WormBase Parasite v. 17.0 and PlanMine v. 3.0 databases (see Table 1 and Online Resource 1, Howe et al., 2017; Rozanski et al., 2019). Gene predictions for the genome of *Proales similis* were performed using Funannotate v. 1.8.11 (see Online Resource 1 for details). Gene-annotation files (GFF) and corresponding FASTA files were processed with custom scripts to remove pseudogenes, alternative transcripts or isoforms, and tRNA genes before orthology

prediction. The filtered gene annotations and corresponding FASTA files are provided in the supplementary files (see data availability section). Transcriptomic reads for *L. maerski* were downloaded from the NCBI-SRA database and were subsequently trimmed and assembled with Trinity v. 2.14.0 (see Online Resource 1, Grabherr et al., 2011). The assembled transcripts were used as input for TransDecoder v. 5.5.0 to predict a credible set of protein sequences for downstream analyses (see Online Resource 1 and Table 1). Gene completeness of protein datasets was inferred using universal single-copy orthologs (BUSCO) v. 5.2.2 (Manni et al., 2021, Table 1, Online Resource 1: Fig. S1).

### Orthology prediction, single-copy ortholog set construction, and supermatrix generation

Orthology prediction using the 12 species' proteomes was performed with Orthofinder v. 2.5.4 with the options: -M msa -T raxml-ng (Emms & Kelly, 2019; Kozlov et al., 2019). The results of orthology prediction showed that only 101 orthogroups (OGs) contained single-copy genes across all species. This could be partially due to the whole-genome duplication event in the stem lineage of bdelloid rotifers (Mark Welch et al., 2008; Hur et al., 2009), which could place bdelloid-specific gene duplications (i.e., homoeologs) in the same OG. The presence of uncollapsed haplotypes in genome assemblies or the overall low total number of genes in the genomes of *Proales similis* (Monogononta), *Seison nebaliae* (Seisonidea), and *Pomphorhynchus laevis* (Acanthocephala) could be additional reasons. To increase the total number of genes for phylogenomic analyses, we therefore proceeded by inferring different sets of single-copy orthogroups (SCOGs) using different methodological approaches, starting from the initial OGs inferred by Orthofinder (see Table 2, Online Resource 1: Fig. S2–S4). In the first approach, we selected SCOGs that included at least 10 out of the 12 species to create supermatrix A (Table 2, Online Resource 1: Fig. S2). In the second approach, we first selected SCOGs that contained at least one species from each of the six taxonomic groups whose phylogenetic relationships we wanted to address (Acanthocephala, Bdelloidea, Monogononta, Seisonidea, Micrognathozoa, Platyhelminthes). This set of genes is called taxonomically “decisive” and contained 177



**Table 2** Overview, statistics, and description of amino-acid supermatrices analyzed in the present study. Note that the number of genes refers to the original supermatrices before trimming hypervariable sites (i.e., for supermatrix E)

or removing columns with private/unique amino acids (see also Fig. 2). More detailed statistics are given in the Online Resource 2: Table S1. PI: parsimony-informative sites, OG: orthogroup, SCOG: single-copy orthogroup

Supermatrix ID	No. of species	No. of genes	No. of alignment sites	No. of PI sites	Description
supermatrix A	12	345	86,409	43,019	We selected SCOGs with minimum of 10 species present
supermatrix B	12	233	56,310	28,560	We selected decisive SCOGs (i.e., with $\geq 1$ species from each taxonomic group). Added decisive genes with species-specific gene multiplications only in one non-bdelloid species (max. five copies; we kept the copy with the highest average pairwise non-ambiguous coverage in the alignments)
supermatrix C	12	267	86,214	37,560	We extracted SCOGs from decisive multi-copy OGs using orthoSNAP (requirements: max. five copies per species in each multi-copy OG and min. 10 species in each extracted SCOG)
Supermatrix D	12	262	79,411	38,043	We extracted decisive multi-copy OGs for which only bdelloids have multiple copies. We used OrthoSNAP to extract SCOGs within bdelloid clade and merged the sequences of one of these SCOGs with the single copies of non-bdelloid species in the same OG
Supermatrix E	12	1,200	206,917	120,319	Original supermatrix used by Orthofinder after trimming it with BMGE (all OGs for which at least 66.6% of species are single-copy)
Supermatrix F	10	1,200	206,917	95,141	After removal of the two species of Platyhelminthes from supermatrix E
Supermatrix G	10	1,200	65,508	23,768	After removal of all alignment sites with unique amino acids for any species from supermatrix F
Supermatrix H	10	1,200	162,015	45,201	After removal of sites with unique amino acids for <i>S. nebaliae</i> and/or <i>P. laevis</i> from supermatrix F (only if there were no unique amino-acids for additional species on the same column)
Supermatrix I	10	1,200	146,698	64,394	After removal of sites with unique amino acids for any of the species from supermatrix F (only if no additional species had unique amino acids in the same column)
supermatrix A50.1	12	50	17,007	6,558	After keeping only the best 50 genes from supermatrix A using genesortR
supermatrix A50.2	10	50	17,007	5,057	After removal of the two species of Platyhelminthes from supermatrix A50.1
supermatrix A50.3	10	50	14,303	4,195	After removal of sites with unique amino acids for <i>S. nebaliae</i> and/or <i>P. laevis</i> from supermatrix A50.2
supermatrix B50.1	12	50	17,184	7,265	After keeping only the best 50 genes from supermatrix B using genesortR
supermatrix B50.2	10	50	17,184	5,741	After removal of the two species of Platyhelminthes from supermatrix B50.1
supermatrix B50.3	10	50	13,839	4,578	After removal of sites with unique amino acids for <i>S. nebaliae</i> and/or <i>P. laevis</i> from supermatrix B50.2
supermatrix C50.1	12	50	22,100	7,280	After keeping only the best 50 genes from supermatrix C using genesortR

**Table 2** (continued)

Supermatrix ID	No. of species	No. of genes	No. of alignment sites	No. of PI sites	Description
supermatrix C50.2	10	50	22,100	5,658	After removal of the two species of Platyhelminthes from supermatrix C50.1
supermatrix C50.3	10	50	19,990	5,051	After removal of sites with unique amino acids for <i>S. nebaliae</i> and/or <i>P. laevis</i> from supermatrix C50.2
supermatrix D50.1	12	50	16,271	5,959	After keeping only the best 50 genes from supermatrix D using genesortR
supermatrix D50.2	10	50	16,271	4,629	After removal of the two species of Platyhelminthes from supermatrix D50.1
supermatrix D50.3	10	50	12,884	3,524	After removal of sites with unique amino acids for <i>S. nebaliae</i> and/or <i>P. laevis</i> from supermatrix D50.2

SCOGs (Dell’Ampio et al., 2014). We subsequently added to this set all decisive multi-copy OGs with species-specific gene multiplications after keeping only one copy per species (see supermatrix B, only OGs with multiple copies in only one non-bdelloid species were considered at this step, see Table 2 and Online Resource 1: Fig. S2). In the third approach, we used OrthoSNAP v. 0.1.1 to identify SCOGs within larger multi-copy OGs (minimum number of species required for each SCOGs: 10, supermatrix C, Table 2, Online Resource 1: Fig. S2, see Steenwyk et al., 2022). Lastly, we inferred one set of SCOGs to account for the ancient whole-genome duplication event in bdelloid rotifers (Mark Welch et al., 2008; Hur et al., 2009). Specifically, we first selected taxonomically decisive OGs that had multiple gene copies only in one or more bdelloid species (Online Resource 1: Fig. S2). The subtrees of bdelloid sequences were then extracted from the pre-inferred OG trees of Orthofinder using ETE v. 3.1.2 (Huerta-Cepas et al., 2016). Subsequently, we searched for SCOGs within the extracted bdelloid subtrees using the same version of OrthoSNAP as above (min. number of species required: 4). The bdelloid sequences of the extracted SCOGs were then combined with the single-copy sequences of non-bdelloid species in the same OG (see supermatrix D, Table 2, Online Resource 1: Fig. S2). By using these semi-independent approaches to SCOG selection, we reduced the possibility of biased phylogenetic estimates due to hidden paralogy in some SCOG sets (Emms & Kelly, 2019; Siu-Ting et al., 2019). The custom python

scripts that were used for generating the different ortholog sets from the output of Orthofinder are provided on github (see data availability).

Supermatrices were assembled and analyzed only at the amino-acid sequence level. Before inferring multiple sequence alignments (MSAs), we used PREQUAL v. 1.02 to screen each of the previously inferred SCOGs and mask potentially non-homologous and erroneous amino-acid sequence segments (Whelan et al., 2018). This type of segment filtering has been shown to improve branch-length estimation in molecular phylogenetics (Di Franco et al., 2019) and is relevant for inferring an accurate phylogenetic tree of Syndermata that is often characterized by high levels of branch-length heterogeneity (e.g., Struck et al., 2014; Laumer et al., 2015). Amino-acid sequences in each SCOG were aligned using the software FSA v. 1.15.9 (option: -fast) that greatly reduces false positive alignments and therefore increases the overall accuracy of MSAs (Bradley et al., 2009). We subsequently used BMGE v. 1.12 (options: -h 0.5 -m BLOSUM62) to remove hypervariable alignment columns from the individual MSAs (Criscuolo & Gribaldo, 2010; Vasilikopoulos et al., 2021a). The filtered MSAs of the different sets of SCOGs were then concatenated into four different supermatrices using PhyKIT v. 1.11.7 (supermatrices A, B, C, and D in Table 2 and Online Resource 1: Fig. S2; Steenwyk et al., 2021). We also analyzed the original supermatrix generated by Orthofinder after trimming it with the same version of BMGE as described above (see Table 2, BMGE-trimming resulted in supermatrix E). The



original Orthofinder supermatrix was constructed internally by Orthofinder after selecting OGs for which at least 66% of the species in the dataset were in single copy (Emms & Kelly, 2019).

Selecting subsets of genes, alignment sites, and species for downstream sensitivity analyses

Several approaches have been used to select the optimal subsets of genes and sites for phylogenomic analyses that rely on different criteria (Misof et al., 2013; Salichos & Rokas, 2013; Klopstein et al., 2017; Naser-Khdour et al., 2019; McCarthy et al., 2023). We applied genesortR (version 12.10.2022) on supermatrices A, B, C, and D to select subsets of the 50 most reliable loci from each supermatrix (supermatrices A50.1, B50.1, C50.1, and D50.1; Mongiardino Koch, 2021). GenesortR performs multivariate analyses of several gene properties and attempts to find a PCA axis of usefulness along which proxies for phylogenetic signal increase whereas proxies for systematic bias decrease. GenesortR requires a species tree as input for estimating Robinson-Foulds distances of gene trees to the species tree. This distance is used as a proxy for phylogenetic signal of the genes. However, this presupposes that the species tree is known a priori. To avoid selecting genes that favor a specific topology of syndermatan relationships, we used a tree topology for which the relationships of the major syndermatan groups were collapsed into a polytomy. Individual gene trees for each SCOG were estimated independently and were then provided to the genesortR script (see Online Resource 1).

Since outgroup selection was previously shown to affect phylogenetic inference of Syndermata, we also tested whether removing the two distantly related species of Platyhelminthes affected the inferred syndermatan relationships. Specifically, we removed the two flatworm species from supermatrices A50.1, B50.1, C50.1 and D50.1 and E to generate five additional supermatrices that contained *L. maerski* as the outgroup (Fig. 1a, Table 2, supermatrices: A50.2, B50.2, C50.2, D.50.2, F). Moreover, since we observed extreme branch-length heterogeneity within Syndermata and possible heterogeneous sequence divergence for the acanthocephalan species *P. laevis* (Figs. 1d, 1e, see below for results of the AliGROOVE analysis), we subsequently applied an alignment-site removal strategy to homogenize

branch lengths within the ingroup, generating supermatrices A50.3, B50.3, C50.3, D.50.3, H (Fig. 1a, Table 2). This is because previous studies have shown that selecting a closely related outgroup should be accompanied by taking into account the properties of the ingroup and outgroup taxa as well (Borowiec et al., 2019; Vasilikopoulos et al., 2021a). Because the inclusion of Platyhelminthes in phylogenetic analyses seemed to have had an impact on the internal topology of Syndermata, we only applied this site-removal strategy to supermatrices from which the two species of Platyhelminthes had been previously removed (Fig. 1a, Table 2, supermatrices A50.2, B50.2, C50.2, D.50.2, F). To be more specific, we deleted alignment columns with unique amino-acid residues for *Seison nebaliae* (Seisonidea), *Pomphorhynchus laevis* (Acanthocephala), or for both species from these supermatrices using custom python scripts. Alignment columns were not removed if additional species in the same column also had a unique amino acid to avoid eliminating too many informative sites. Using supermatrix F (that was larger in terms of alignment positions) as input, we also performed two additional filterings: (1) by deleting all columns that included any number of unique amino-acid residues (supermatrix G) and (2) by deleting columns with unique amino-acid residues in only 1 of all the species in the alignment (supermatrix I).

Measuring data completeness, deviation from compositional homogeneity, and other statistical properties of amino-acid supermatrices

Most of the commonly used models of molecular evolution assume that sequences have evolved under stationary, homogeneous, and reversible conditions (SRH conditions, Ababneh et al., 2006; Jermini et al., 2008). If the data violate these assumptions, there is an increased chance for erroneous phylogenetic estimates using these models (Ababneh et al., 2006; Jermini et al., 2008; Naser-Khdour et al., 2019). To measure the degree of deviation from compositional homogeneity among species in each analyzed supermatrix, we inferred relative composition frequency variability values (RCFV, Online Resource 2: Table S1) with BaCoCa v. 1.109 (Zhong et al., 2011; Kück & Struck, 2014). Complementary to the RCFV approach, we performed matched-pairs tests of homogeneity for all supermatrices using the Bowker's

symmetry test (Bowker, 1948; Ababneh et al., 2006). Matched-pairs tests of symmetry were performed with Homo v. 2.0 (available from: <https://github.com/ljermiin/Homo.v2.0>, last access 16.11.2022) and heatmaps of pairwise symmetry tests were generated with HomoHeatmapper v. 1.0 (available from: <https://github.com/ljermiin/HomoHeatMapper>, last access 16.11.2022, see Jermiin et al., 2020).

We additionally inferred completeness scores for all supermatrices, heatmaps of pairwise completeness scores, and average pairwise  $p$ -distances using AliStat v. 1.14 (Wong et al., 2020). Lastly, we inferred substitution saturation scores (Philippe et al., 2011), the standard deviation of long-branch scores (LB score standard deviation, Online Resource 2: Table S1, Struck, 2014), and treeness-over-RCV scores (treeness divided by relative composition variability, TORCV, Online Resource 2: Table S1) using the same version of PhyKIT as above (Phillips & Penny, 2003; Steenwyk et al., 2021). Treeness (or ‘stemminess’) of a phylogenetic tree measures the proportion of tree distance on the internal tree branches and can be used as a measure of the signal-to-noise ratio in a phylogeny (Lanyon, 1988; Phillips & Penny, 2003; Steenwyk et al., 2021). Relative composition variability (RCV) measures the amino-acid (or nucleotide) composition variability across species in the underlying MSA (Phillips & Penny, 2003). Higher TORCV scores are therefore desirable, as they are associated with higher signal-to-noise ratio and reduced compositional and other biases (Phillips & Penny, 2003; Steenwyk et al., 2021). The LB score measures for each species the percentage deviation from the average patristic distance across all pairs of species and is a metric that is independent of the root of the tree (Struck, 2014). The standard deviation of LB scores of a phylogenetic tree provides a measure of branch-length heterogeneity (Struck, 2014). Lower standard deviation of LB scores is associated with reduced branch-length heterogeneity and thus reduced potential for long-branch attraction (Struck, 2014). We used the maximum-likelihood trees with the best log-likelihood scores that were inferred under the best-fitting models (see following section) for inferring all tree-dependent statistics for each supermatrix (i.e., saturation scores, standard deviation of LB scores, TORCV values, see Online Resource 2: Table S1). Lastly, we also screened the supermatrices with reduced taxon sampling for evidence of heterogeneous sequence

divergence of individual species with AliGROOVE v. 1.08 (Kück et al., 2014). AliGROOVE maps suspicious branches on a phylogenetic tree based on the pairwise similarity of sequences in the MSA and can facilitate the identification of highly divergent or saturated sequences. Such sequences are often characterized by extremely long branches in inferred phylogenetic trees and might be incorrectly placed in a phylogeny (Kück et al., 2014). Processing and analysis of the properties of supermatrices, species, and trees were performed with pandas v. 1.4.3, while statistical visualization of these properties was performed using matplotlib v. 3.5.1 and seaborn v. 0.11.2 (Hunter, 2007; McKinney, 2010; Waskom, 2021).

Model selection and phylogenetic reconstruction with site-heterogeneous and site-homogeneous substitution models

Phylogenetic reconstructions were performed both in maximum-likelihood and Bayesian frameworks. For maximum-likelihood analysis, we first selected the best-fit substitution model for phylogenetic reconstruction with ModelFinder as implemented in IQ-TREE v. 1.6.12 (Nguyen et al., 2015; Kalyaanamoorthy et al., 2017). Our model selection procedure was performed on unpartitioned supermatrices by including empirical profile mixture models with 61 components (C60+F models) that account for among-site compositional heterogeneity (i.e., site-heterogeneous, see Online Resource 1; Le et al., 2008). In total, 70 models were tested on each supermatrix. Phylogenetic tree reconstructions were performed with the best-fit substitution model for each supermatrix and the same version of IQ-TREE. Since site-heterogeneous models always had a better fit than site-homogeneous models, we also analyzed all supermatrices with the site-homogeneous LG+F+R5 model to test the sensitivity of phylogenetic results to model miss-specification. We performed five independent tree searches with 1) the best-fit model and 2) with the LG+F+R5 model and selected the tree with the best log-likelihood score among the five tree searches as the best maximum-likelihood tree under each model to avoid potential local optima in the analyses (Stamatakis & Kozlov, 2020). IQ-TREE produced a warning that the mixture models might be overfitting because a few mixture weights were estimated close to 0 (despite being selected as the best models). For this reason, we repeated the tree searches for all

supermatrices with a less complex site-heterogeneous profile mixture model (e.g., LG+C20+F+R5, see Online Resource 2: Table S2) and compared the results of phylogenetic reconstructions. Statistical branch support was estimated based on 1000 ultrafast bootstrap replicates (UFB, with the option `-bnni` to avoid inflated branch support due to inadequate modeling) and 2000 SH-aLRT replicates in all cases (Guindon et al., 2010; Hoang et al., 2018).

We also performed Bayesian phylogenetic inference of Syndermata relationships for a selection of supermatrices with the site-heterogeneous CAT+GTR+G4 model as implemented in *phylobayes-mpi* v. 1.9 (see Online Resource 2: Table S2; Lartillot & Philippe, 2004; Lartillot et al., 2013; Lartillot, 2020). Two independent Markov chain Monte Carlo (MCMC) analyses were run for each analyzed supermatrix until convergence. Convergence in the tree space was assessed with *bpcomp* (`maxdiff` < 0.1, default parameters), and we also checked for the convergence of the parameter values with *tracecomp* (a run with an effective size > 50 for all parameters is considered acceptable according to the manual of *phylobayes*). Posterior consensus trees using two chains for each analyzed supermatrix were then produced with *bpcomp* (Lartillot, 2020). All inferred phylogenetic trees were rooted and visualized with *iTOL* v. 6 (Letunic & Bork, 2021). Lastly, we performed posterior predictive checks, in order to assess the adequacy of the GAT+GTR+G4 model to describe 1) across-species compositional heterogeneity and 2) specificity of amino-acid compositions of sites due to biochemical constraints (Bollback, 2002; Feuda et al., 2017; Lartillot 2020). Using these tests, we also monitored the effect of distant outgroup removal on the ability of CAT+GTR+G4 to describe compositional patterns across species and sites in the supermatrices. Posterior predictive checks for i) compositional heterogeneity across species (two summary statistics used: maximum and mean squared heterogeneity, option: `-comp`) and ii) mean site-specific amino-acid diversity (option: `-div`) were performed using the same version of *phylobayes* as above. For performing these posterior predictive checks, we simulated at least 100 datasets from the posterior distribution for supermatrices A50.1, A50.2, B50.1, B50.2, B50.3, C50.1, C50.2, D50.1, D50.2, and D50.3 (Online Resource 2: Table S3).

Comparing properties of supermatrices that support or not the different syndermatan relationships

Since the above-described removal of sites with unique amino acids resulted in improved values concerning statistical properties with putative connection to systematic error (i.e., LB score standard deviation, TORCV), and because not all analyses of filtered datasets resulted in the same syndermatan topology (Fig. 2b), we assessed the plausibility of four hypotheses of syndermatan relationships by evaluating under which conditions each of these hypotheses (or clades) is inferred or not inferred (Fig. 2b, Fig. 3a–3d). The hypotheses that we tested were as follows: 1) monophyly of Acanthocephala+Bdelloidea+Monogononta (i.e., the Seisonidea-sister hypothesis), 2) Acanthocephala is the sister group of Bdelloidea (the Lemniscea hypothesis), 3) monophyly of Acanthocephala+Bdelloidea+Seisonidea (the Hemirotifera or Monogononta-sister hypothesis), and 4) Acanthocephala is the sister group of Seisonidea (the Pararotatoria hypothesis, see Figs. 2b, 3a–3d). We selected these hypotheses based on the results of previous molecular phylogenetic studies but also based on the results of our own analyses. Note that not all tested hypotheses are mutually exclusive, as the Hemirotifera hypothesis is compatible with both the Pararotatoria and the Lemniscea hypothesis. On the other hand, the Seisonidea-sister hypothesis is only compatible with the Lemniscea hypothesis.

Assuming sufficient phylogenetic signal given the size of our supermatrices (> 12,000 amino-acid sites, Table 2), we postulated that inference or not of each these hypotheses is likely due to systematic error in concatenation-based analyses (i.e., inability of the model to accommodate some heterogeneity in the evolutionary process). We further postulated that dataset properties with potential connection systematic error (i.e., TORCV, standard deviation of LB scores and saturation scores) could be used to evaluate these datasets as more or less likely to produce erroneous phylogenetic inferences. More specifically, if datasets supporting a phylogenetic hypothesis have more desirable properties than datasets that do not support it (i.e., higher TORCV, lower standard deviation of LB scores, and higher saturation scores), the given hypothesis is less likely to be artefactual. In contrast, if their properties are less desirable than the properties of datasets that do not support a

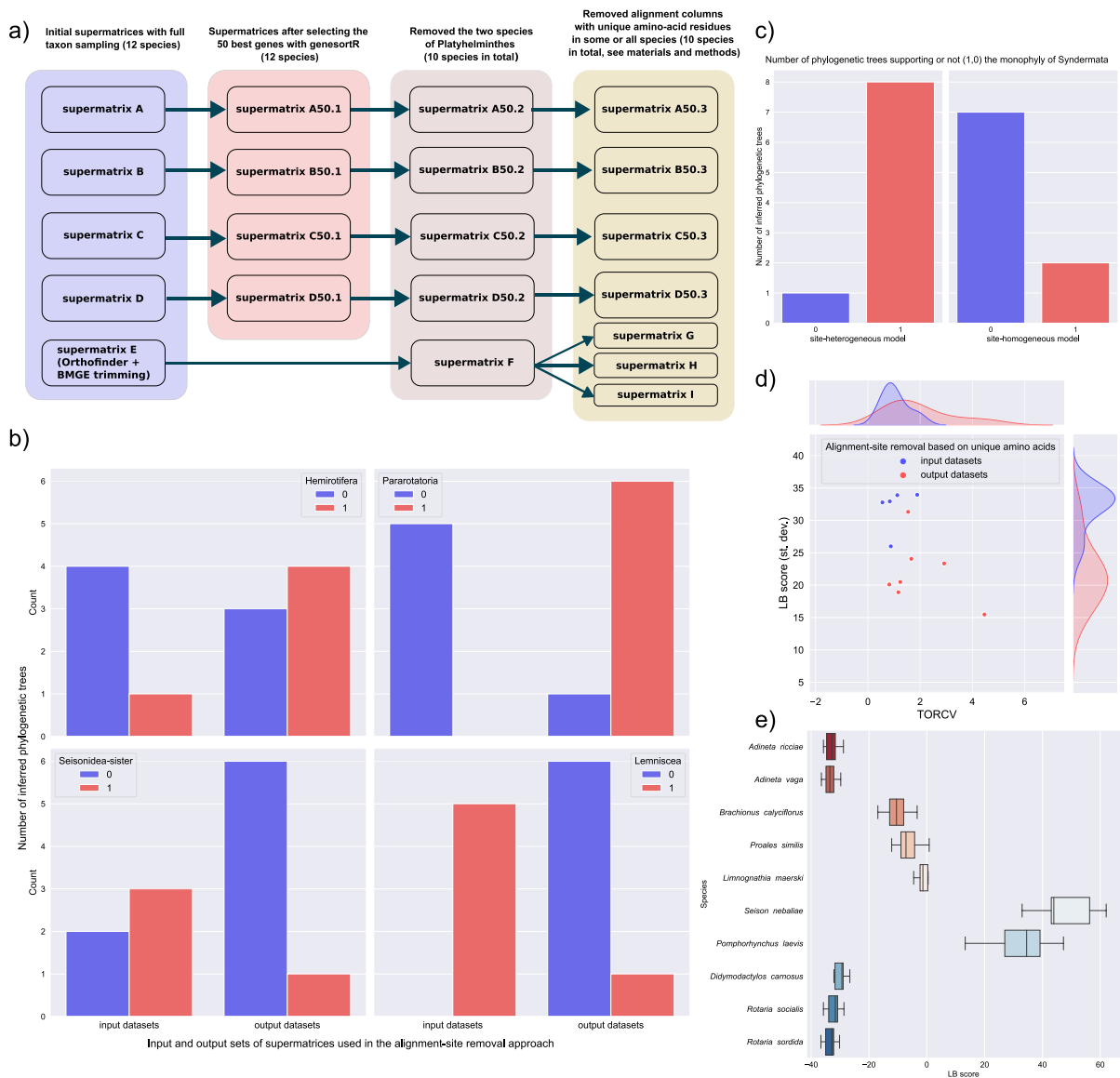


**Fig. 2** **a** Workflow describing the steps for generating the different supermatrices analyzed in the present study (see also Table 2); **b** Summary of phylogenetic results from concatenation-based analyses before and after removing alignment sites with unique amino acids for some or all species (see methods and Table 2). Input datasets are supermatrices before removing sites with private amino-acids (third column in Fig. 2a, five supermatrices: A50.2, B50.2, C50.2, D50.2, F) whereas output datasets are supermatrices after these alignment sites have been removed (fourth column in Fig. 2a, seven supermatrices: A50.3, B50.3, C50.3, D50.3, G, H, I). Results are shown based on the maximum-likelihood trees inferred with the site-heterogeneous model. Support (i.e., inference) or not of the different hypotheses is denoted as 1 and 0, respectively; **c** number of inferred trees supporting or not (1 and 0, respectively) the Syndermata hypothesis depending on the evolutionary model (only supermatrices with full taxon sampling).

Results are based on the maximum-likelihood analyses using the empirical profile mixture model with 61 profiles (site-heterogeneous) and the LG + F + R5 model (site-homogeneous); **d** effect of removing alignment sites with unique amino acids on the properties of inferred trees and supermatrices (input supermatrices are before removing these sites whereas output supermatrices are after removing these sites, see third and fourth column in Fig. 2a). Overall, this site-removal approach results in increased TORCV values and reduced branch-length heterogeneity (LB score standard deviation); **e** extreme branch-length heterogeneity among subgroups of Syndermata. Distribution of LB scores for each species across the different supermatrices (only supermatrices with reduced taxon sampling and before removing sites with unique amino acids are taken into account, see third column in Fig. 2a). LB score: long-branch score; TORCV: treeness divided by relative score composition variability (see methods)

hypothesis, then this hypothesis should be considered less likely. We plotted the median: 1) TORCV score, 2) standard deviation of LB scores, and 3) saturation score separately for a) the datasets that supported and b) the datasets that did not support each of these four hypotheses. These analyses were only performed based on datasets for which species of Platyhelminthes had been removed (supermatrices: F, G, H, I, A50.2, A50.3, B50.2, B50.3, C50.2, C50.3, D50.2, D50.3). Analyses were repeated after excluding the results of supermatrix G, as this was the most stringently trimmed supermatrix, showing extreme values of standard deviation of LB scores (low), TORCV (high), and saturation score (low, Online Resource 1: Fig. S5).

### Species-tree inference from multi-copy orthogroups

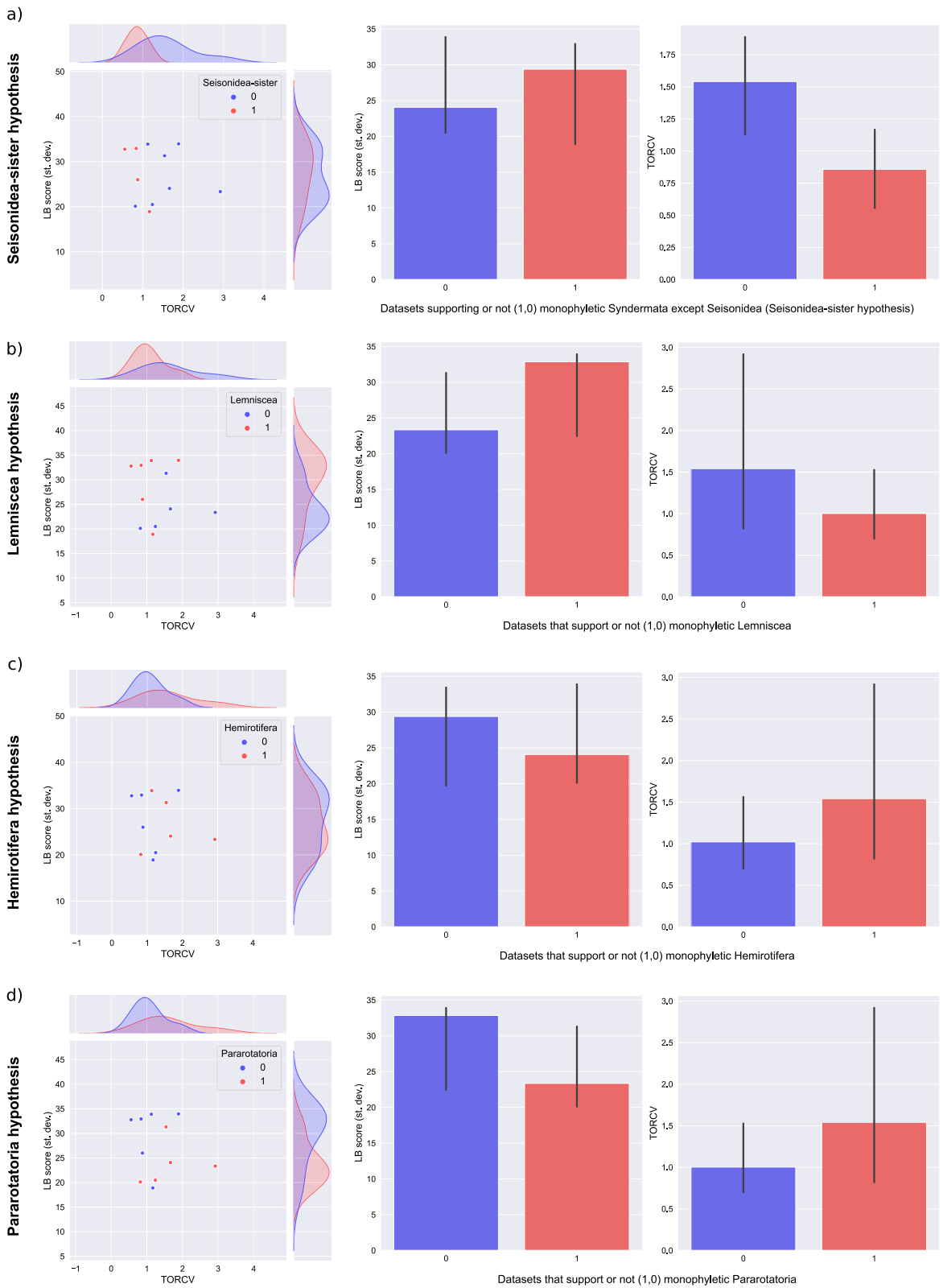
As an alternative approach to the concatenation-based analyses, we applied phylogenomic methods that leverage information from both single- and multi-copy gene families (or OGs). We applied different species-tree methods that take into account different biological sources of gene-tree heterogeneity (Maddison, 1997). First, we selected taxonomically decisive OGs that contained a maximum of five gene copies per species (2,010 OGs, Online Resource 1: Fig. S2). Subsequently, we used the gene trees of these OGs (inferred internally by Orthofinder) for species-tree reconstruction with SpeciesRax that is part of the software package GeneRax v. 2.0.4 (Morel et al., 2020, 2022). SpeciesRax is robust to differential gene duplication and loss but also gene transfer events when inferring a species tree from a set of multi- and single-copy gene trees. We also applied ASTRAL-Pro v. 1.10.1.3 on the same set of gene trees (Zhang & Mirarab, 2022). ASTRAL-Pro has been shown to be statistically consistent under the multi-species coalescent model and can therefore compensate for incomplete lineage sorting (Zhang et al., 2020; Zhang & Mirarab, 2022). Lastly, we applied the species-tree inference method that is implemented in STAG v. 1.0.0 (Emms & Kelly, 2018). STAG computes the shortest inter-species distances in the individual OG trees to construct distance matrices and species trees for each OG and therefore takes into account only OGs that include at least one gene copy from each species in the dataset. This collection of preinferred species trees is then used to infer a greedy consensus

species tree from all OGs that contain all species (Emms & Kelly, 2018, 2019). Since the STAG method can only process OGs that contain all species in the putative species tree, the number of OGs was reduced from 2,010 to 1,479 for the initial STAG analysis. When the two species of Platyhelminthes were removed from the initial 2,010 OGs, the number of informative OGs was reduced from 2,010 to 1,628 for the same analysis.

Since individual OG trees were inferred by default using the LG + G4 model within the Orthofinder pipeline, we tested whether selecting the best-fit model for inferring the OG trees affected the downstream species-tree inference. We selected the best-fit substitution model for each OG using the Orthofinder MSAs and IQ-TREE v. 1.6.12 (AICc criterion, see Online Resource 1 for detailed commands). Phylogenetic tree reconstruction for each preinferred MSA was then performed with the same version of IQ-TREE. Species-tree reconstructions were repeated using the same versions of GeneRax, ASTRAL-Pro, and STAG as above. Using the OG trees that were derived with the best-fit models, we also selected and analyzed subsets of the best OG trees with 1) increased signal-to-noise ratio and reduced compositional bias (highest TORCV scores) and 2) reduced branch-length heterogeneity (lowest standard deviation of LB scores). For each of the two subsampling strategies, we analyzed a) the top 50% (1,005 of 2,010) and b) the top 500 genes. TORCV values and LB standard deviation scores for each gene tree were calculated with the same version of PhyKIT as described above. Because of previous claims that the internal phylogeny of Syndermata is negatively affected by using a distantly related outgroup, we also checked whether removing all sequences of Platyhelminthes from the OGs affected the phylogenetic results of species-tree methods. For doing this, we removed the two species of Platyhelminthes from all previously selected MSAs of OGs, re-inferred gene trees, and repeated all species-tree reconstructions as described above.

### Microsynteny-based phylogenetic reconstruction of Syndermata

As a last approach to species-tree inference, we performed microsynteny-based phylogenetic reconstructions with the software package syntenet v. 1.0.2 using R v. 4.2.2 (R Core Team, 2021; Almeida-Silva





◀**Fig. 3** Evaluation of the species-tree and supermatrix properties that supported or not (1 or 0, respectively) the four selected phylogenetic hypotheses within Syndermata. Left: supermatrices (dots) are plotted in the 2D space based on 1) the branch-length heterogeneity of their inferred trees (standard deviation of LB scores) and 2) TORCV scores. Right: barplots show median values of LB score standard deviation and median TORCV values separately for the supermatrices whose analyses resulted in the inference or not (1, 0) of each hypothesis. **a** Seisonidea-sister hypothesis (i.e., monophyly of Acanthocephala + Bdelloidea + Monogononta); **b** Lemniscea hypothesis; **c** Hemirotifera hypothesis; **d** Pararotatoria hypothesis

et al., 2023). For this analysis, we used as input the GFF and proteome files of all genomes in our dataset (all species except *L. maerski*, see Table 1). First, all-versus-all BLASTp searches for the input proteomes were performed with DIAMOND v. 2.0.13.151 within the syntenet R package (Buchfink et al., 2021). The BLAST results and the genomic coordinates of genes were automatically used to infer synteny network across all genomes using a version of MCSanX that is implemented within syntenet (Wang et al., 2012; Almeida-Silva et al., 2023). We used three different combinations of parameters for defining syntenic blocks and repeated all phylogenetic analyses below for each parameter combination: i) max\_gaps=60 and anchors=2, ii) max\_gaps=60 and anchors=3, iii) max\_gaps=80 and anchors=2. These relaxed parameters for identifying syntenic blocks were used because it was previously shown that the microsynteny approach might work better with more permissive synteny parameters in distantly related taxa (Zhao et al., 2021), and because the genomes of Syndermata showed reduced levels of deeply conserved synteny. Subsequently, we performed clustering of the synteny network and performed phylogenomic profiling of the clusters to identify which of them are present in which phylogenetic groups using the provided functions within the package syntenet. Absence or presence of the inferred synteny clusters across species was then used to perform microsynteny-based species-tree reconstruction. Specifically, the phylogenomic profiles across species were converted to a supermatrix of binary characters (0, 1) for phylogenetic analysis. A different supermatrix was produced for each set of synteny-block definition parameters. The binary data were treated as discrete morphological characters for phylogeny estimation in a maximum-likelihood framework (option: -st MORPH in IQ-TREE). Best-fit substitution models

for the binary-data supermatrices were selected using default options in ModelFinder (option: -m MFP) and phylogenetic trees were inferred using IQ-TREE v. 1.6.12. Statistical branch support was assessed with 1,000 UFBs (option: -bnni) and 2,000 SH-aLRT replicates. The phylogenetic trees were rooted and visualized with iTOL v. 6 after omitting branch lengths in order to show only the species-tree topology (Letunic & Bork, 2021). Our microsynteny-based phylogenetic approach did not include *L. maerski*, as whole-genome data were not available for this species.

We also used site-concordance factors to estimate discordance of phylogenomic signal in the microsynteny data with respect to the two competing hypotheses of early syndermatan relationships (Monogononta-sister vs. Seisonidea-sister hypotheses, Minh et al., 2020a; Mo et al., 2023). The site-concordance factor is defined as the percentage of informative alignment sites (i.e., in this case microsynteny clusters) supporting a branch in the reference tree (averaged over all quartets around this branch). We estimated site-concordance factors using both parsimony and maximum-likelihood methods (SCF and SCFL, respectively, Minh et al., 2020a; Mo et al., 2023) and by using all possible quartets. Site-concordance factors for the Monogononta-sister (i.e., Hemirotifera) hypothesis were inferred by providing the preinferred species-tree topologies to IQ-TREE. Calculation of site-concordance factors in support of the Seisonidea-sister hypothesis (i.e., a clade that includes Bdelloidea + Monogononta + Acanthocephala) was performed by supplying a fixed tree topology to IQ-TREE for which *Seison nebaliae* was placed as sister to all other syndermatan species, leaving the rest of the phylogenetic relationships unchanged. All site-concordance factor analyses were performed with IQ-TREE v. 2.2.2 (Minh et al., 2020b).

## Results

### Orthology prediction and ortholog-set selection

The orthology prediction analysis with Orthofinder resulted in a total number of 273,614 genes from 12 species being assigned to 31,139 OGs (~90.5% of genes were assigned to OGs). A total of 8,594 OGs were species-specific (i.e., contained genes of only one species). In contrast, 28,832 genes were

not assigned to any OG (~9.5% of genes). The Orthofinder analysis also produced a set of 101 SCOGs, each composed of single-copy genes from every species in the analysis. Since this number of SCOGs was considered relatively low for phylogenetic analysis, we did not directly use this set of SCOGs for downstream phylogenomic inference. However, extracting all SCOGs that contained at least 10 out of 12 species from the output of Orthofinder resulted in an increased number of SCOGs ( $n=345$ , supermatrix A, Fig. 2a, Table 2, Online Resource 1: Fig. S2).

Using the output of Orthofinder, we additionally identified 2,010 decisive OGs that contained at least one species from each focal taxonomic group (Acanthocephala, Bdelloidea, Monogononta, Seisonidea, Micrognathozoa, Platyhelminthes) and maximum five gene copies per species (Online Resource 1: Fig. S2). Starting from this set of OGs, the remaining sets of SCOGs were inferred (i.e., ortholog sets). These sets were the basis for assembling supermatrices B, C, and D (Online Resource 1: Figs S1–S4). More specifically, combining a) decisive SCOGs (i.e., with  $\geq 1$  species from each taxonomic group) with b) decisive OGs that had species-specific gene duplications in only one non-bdelloid species resulted in 233 SCOGs (ortholog set of supermatrix B, Fig. 2a, Table 2, Online Resource 1: Fig. S2). The OrthoSNAP analysis resulted in 267 single-copy subgroups of OGs being extracted from the above-mentioned set of 2,010 OGs (ortholog set for supermatrix C, Table 2, Online Resource 1: Fig. S2). Lastly, after extracting OGs with gene duplications only in bdelloid rotifers and controlling for reduced missing data, we inferred an additional set of 262 SCOGs (ortholog set for supermatrix D, Table 2, Online Resource 1: Fig. S2). Overlap analyses of these ortholog sets showed that they were semi-independent with varying degrees of OG overlap (Online Resource 1: Figs. S3, S4). Specifically, the ortholog sets of supermatrices C and D did not share any OGs with the ortholog set of supermatrix A, whereas the ortholog sets of supermatrices A and B showed the highest OG overlap (168 shared OGs). Lastly, Orthofinder produced an amino-acid supermatrix based on 1,200 OGs that contained single-copy genes for the majority of species (66.6% of species, 8 of the 12 species, supermatrix E before trimming, Table 2).

Supermatrix E was the largest in terms of amino-acid alignment sites even after applying the BMGE trimming (206,917 amino-acid alignment sites, see Table 2).

#### Statistical properties of different species, amino-acid supermatrices, and their inferred trees

We observed extreme branch-length heterogeneity within Syndermata as indicated by the LB scores of specific species in the analyzed supermatrices (e.g., Fig. 2e, Online Resource 1: Fig. S6). Overall, species of Bdelloidea and Monogononta showed much lower LB scores in comparison with Acanthocephala and Seisonidea. Specifically, *P. laevis* and *S. nebaliae* were the two species of the ingroup with the highest LB scores when considering all supermatrices under both site-heterogeneous and site-homogeneous models (Fig. 2e, Online Resource 1: Fig. S6). These two species had the highest LB scores, irrespective of whether species of Platyhelminthes were included in the phylogenetic analysis (Fig. 2e, Online Resource 1: Fig. S6).

Amino-acid completeness score was high across supermatrices (ranging from 83.3% to 94.6%) with *P. laevis* being the species with the highest degree of missing data in most datasets (Online Resource 1: Figs. S7–S27, Online Resource 2: Table S1). Screening of the supermatrices and the corresponding inferred trees with AliGROOVE did not show the evidence for clades being supported due to strong heterogeneous sequence divergence irrespective of the topology obtained (Online Resource 1: Figs. S28–S43). Nevertheless, individual sequences of *P. laevis* showed evidence of potential heterogeneous sequence divergence in the similarity-based colored heatmaps and corresponding color-mapped trees produced by AliGROOVE (Online Resource 1: Figs. S28–S43). However, this could also be due to the high proportion of missing data for *P. laevis* in some of the analyzed supermatrices (e.g., supermatrices A, A50.1, A50.2, E, F, H, Online Resource 1: Figs. S7, S11, S12, S14, S16, S17, S28–S31, S38–S43).

In an attempt to reduce the possibility for phylogenetic artifacts due to excessive branch-length heterogeneity, we applied a site-removal strategy based on the presence of unique amino acids for some or all species (see methods). Our site-removal strategy resulted in improved levels of branch-length

heterogeneity in the analyzed datasets (lower standard deviation of LB scores) and also increased TORCV values (Fig. 2d, Online Resource 2: Table S1). Such conditions of data and tree properties are desirable for avoiding artifacts due to systematic errors. In addition, the above-mentioned site-removal strategy resulted in a reduced proportion of failed symmetry tests of compositional homogeneity in some datasets, showing less potential deviation from model assumptions in these filtered supermatrices (supermatrices: B50.3, C50.3, D50.3, see Online Resource 1: Figs. S44–S64 and Online Resource 2: Table S1). Nevertheless, it is unclear whether this reduced proportion of failed symmetry tests for compositional homogeneity was due to the smaller alignment length of the filtered supermatrices, as the proportion of failed pairwise tests was positively correlated with the size of the dataset (i.e., number of alignment sites, Pearson's  $r$ : 0.82,  $p$ -value=0.00093, Online Resource 1: Figs. S65–S67).

Topology of Syndermata is dependent on the choice of substitution model in concatenation-based analyses under full taxon sampling

Our model selection procedure always identified empirical profile mixture models as best-fitting for all supermatrices (Online Resource 2: Table S2). More specifically, the LG+C60+F+R5 model was most commonly selected as the best-fit model across supermatrices (Online Resource 2: Table S2). We observed that this choice of substitution model affected the inferred relationships within Gynognathifera (i.e., Micrognathozoa+Syndermata) when Platyhelminthes were included in the analyses (Fig. 2c, Online Resource 1: Figs. 68–129). Overall, Syndermata was recovered as sister to Micrognathozoa with strong support when using a model that accounts for compositional heterogeneity across sites (Fig. 2c, eight of nine supermatrices under full taxon sampling models: LG+C60+F+R5, WAG+C60+F+R5). In contrast, when using a site-homogeneous model for phylogenetic reconstruction, we inferred Micrognathozoa nested within Syndermata in seven out of nine cases (Fig. 2c, model: LG+F+R5). In all these cases, Seisonidea was placed as sister to a clade Micrognathozoa+(Acanthocephala+Bdelloidea+Monogononta). Using an empirical profile mixture model, with 21 instead of 61 amino-acid

profiles (i.e., LG+C20+F+R5, Online Resource 2: Table S2), also favored the Syndermata hypothesis (seven out of nine supermatrices, Online Resource 1: Figs. S109–129). Additionally, all but one Bayesian phylogenetic analyses of supermatrices with full taxon sampling and the CAT+GTR+G4 model also supported the Syndermata with high posterior probability (three out of four analyses, Online Resource 1: Figs. S130–S140). In summary, for the majority of cases, the Syndermata hypothesis could not be inferred unless a model that accounts for among-site compositional heterogeneity was applied (supermatrices A, A50.1, B, C, D, D50.1). We observed, however, that for two supermatrices, the Syndermata hypothesis was inferred under both optimal and sub-optimal evolutionary models (site-homogeneous and site-heterogeneous, supermatrices E and B50.1).

Phylogeny of the major subclades of Syndermata inferred from concatenation-based analyses

Maximum-likelihood phylogenetic analyses with the empirical profile mixture models resulted in Seisonidea placed as sister to all other lineages of Syndermata for seven out of the nine supermatrices under full taxon sampling (see Online Resource 1: Figs. S68–S87, LG+C60+F+R5, WAG+C60+F+R5). However, the clade Acanthocephala+Bdelloidea+Monogononta (i.e., Fig. 1e) did not receive strong branch support in all maximum-likelihood analyses (e.g., supermatrices: A50.1 with 85% UFB support, and B50.1 with 51% UFB support). Selection of the top 50 genes for phylogenetic analysis did not affect this phylogenetic relationship under the same empirical profile mixture models but support of a clade Acanthocephala+Bdelloidea+Monogononta was then greatly reduced (e.g., from 99% UFB support in supermatrix A to 85% UFB support in supermatrix A50.1, Online Resource 1: Figs. S68, S69). Moreover, removal of the distantly related Platyhelminthes from the analyses resulted in Monogononta placed as sister to the rest of Syndermata when analyzing supermatrix F, or as sister to Seisonidea when analyzing supermatrix B50.2 (with low SH-aLRT and UFB support, Online Resource 1: Figs. S74, S85). Furthermore, the branch support in favor of monophyletic Acanthocephala+Bdelloidea+Monogononta (i.e., Seisonidea-sister hypothesis) was reduced when removing Platyhelminthes from supermatrices

A50.1, C50.1, and D50.1 (e.g., from 85% in A50.1 to 65% UFB support in A50.2, and from 94% UFB in C50.1 to 63% UFB in C50.2). These observations show 1) reduced branch support for the Seisonidea-sister hypothesis when selecting a subset of the most reliable genes for analysis as selected based on the criteria used by genesortR and 2) reduced branch support or lack of support for the Seisonidea-sister hypothesis when excluding amino-acid sequences of the distantly related Platyhelminthes from the phylogenetic analysis.

Since the above-mentioned observations indicated potential attraction of *S. nebaliae* to the distantly related Platyhelminthes, and because our complementary phylogenetic approaches suggested Monogononta (and not Seisonidea) as sister to all other lineages of Syndermata (see below for the microsynteny-based analyses), we also looked at the effect of removing

alignment sites with unique amino acids on the internal phylogeny of Syndermata (see methods, Fig. 2a). For supermatrices B50.3, D50.3, and H, I, this alignment-site removal recovered the Pararotatoria hypothesis within Hemirotipera (i.e., the Monogononta-sister hypothesis, Fig. 4). The Pararotatoria, but not Hemirotipera, hypothesis was also supported by the analysis of the most stringently filtered dataset (supermatrix G, note: Hemirotipera was nevertheless inferred under the less complex LG+C20+F+R5 model in the analysis of supermatrix G). Despite this, removal of alignment sites with unique/private amino acids for *P. laevis* and *S. nebaliae* did not alter the topology in the analyses of supermatrix C50.3 that supported Seisonidea as sister to all other Syndermata although with low UFB support (60%, Online Resource 1: Fig. S79). Removing sites with unique amino acids for *P. laevis* and *S. nebaliae* from supermatrix A.50.2 resulted in

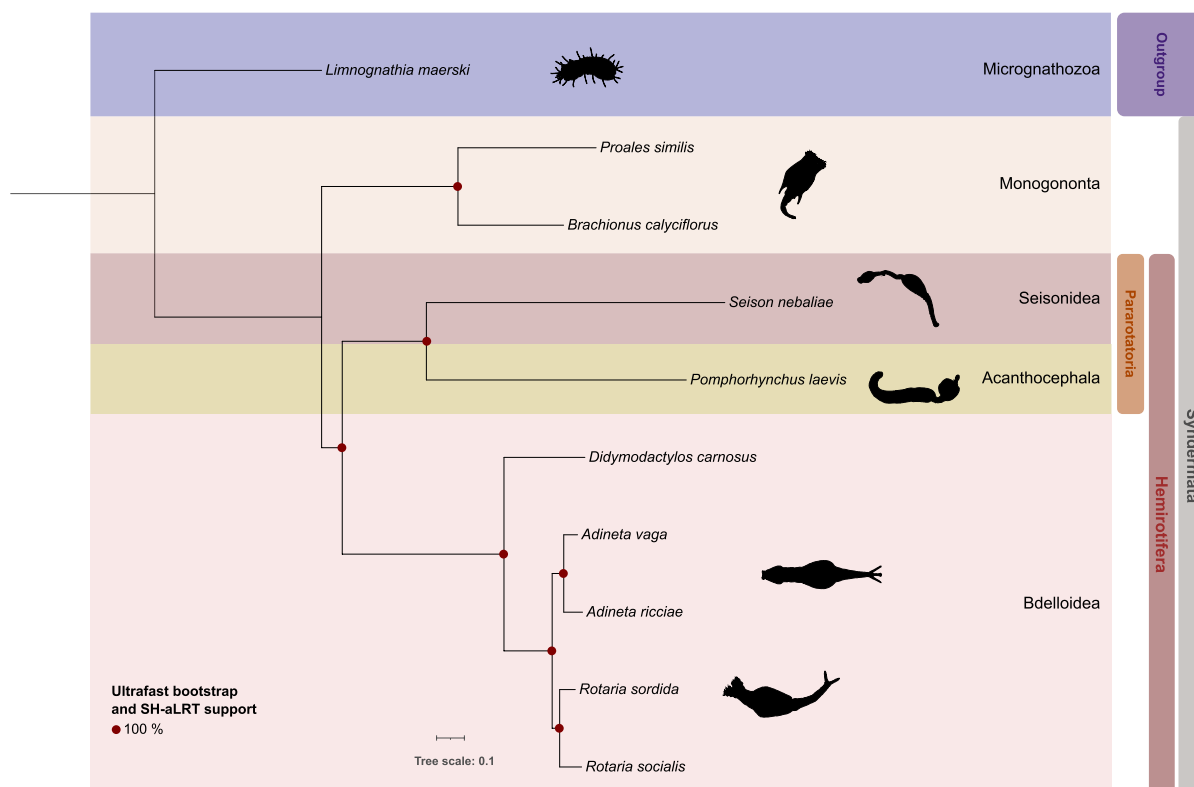


**Fig. 4** Phylogenetic tree with the best log-likelihood score that resulted from the maximum-likelihood phylogenetic analysis of supermatrix H using the LG+C60+F+R5 model. The tree was rooted with the micrognathozoan *Limnognathia maerski*. Statistical branch support is shown on the tree nodes on

2,000 SH-aLRT and 1,000 ultrafast bootstrap and replicates. This phylogenetic tree displays features associated with more reliable combinations of data and methods across concatenation-based analyses

the recovery of Eurotatoria (Fig. 1c, Online Resource 1: Fig. S71) with low statistical branch support (79% UFB support). This was the only dataset whose analyses resulted in Pararotatoria placed as sister to Eurotatoria when using a site-heterogeneous model (but see also analysis of supermatrix G under LG+F+R5, Online Resource 1: Fig. S94). Overall, we observed that our strategy of removing sites with unique amino acids from the analyzed supermatrices resulted in 1) an increased proportion of analyses that supported the Hemirotifera and Pararotatoria hypotheses (4/7 and 6/7 of filtered supermatrices, respectively, for each hypothesis, Fig. 2b) and 2) a reduced proportion of supermatrices that supported the Seisonidea-sister and Lemniscea hypotheses (only 1/7 of filtered supermatrices for each hypothesis, respectively, Fig. 2b).

#### Assessing model adequacy in Bayesian phylogenetic analyses with posterior predictive checks

We performed posterior predictive analyses to assess model adequacy with respect to two dataset properties: (a) across-species compositional heterogeneity and (b) mean site-specific amino-acid diversity. Our results show that the CAT+GTR+G4 model adequately described mean site-specific amino acid diversity in the supermatrices, since the predicted values of mean site-specific amino-acid diversity did not significantly deviate from the observed values in the supermatrices (e.g., posterior predictive  $p$ -values for supermatrices B50.1, B50.2, B50.3: 0.13, 0.24, and 0.26, respectively, see Online Resource 2: Table S3). In addition, we observed that the  $|z|$  score for the same statistic (absolute number of standard deviations of the mean observed value from mean of predicted values) decreased after removing the two species of distantly related Platyhelminthes (see  $|z|$  scores for mean site-specific amino-acid diversity in supermatrices A50.2, B50.2, C50.2, D50.2). The model was, therefore, better able to predict mean site-specific diversity of amino acids after removing flatworms from our phylogenetic analyses.

In contrast, the majority of posterior predictive checks for compositional heterogeneity across taxa showed that the CAT+GTR+G4 model does not adequately capture this type of heterogeneity in the supermatrices (but see maximum compositional heterogeneity statistic for supermatrices D50.1, D50.2, D50.3). We observed, however, that  $|z|$  scores for

mean squared compositional heterogeneity decreased for all supermatrices after removing the two species of Platyhelminthes. A similar pattern was observed when using maximum compositional heterogeneity across species as a statistic with the exception of supermatrix B50.2 (see Online Resource 2: Table S3). Reduced  $|z|$  scores show that removing these two species results in weaker rejection of the null hypothesis (that the model adequately captures across-species compositional heterogeneity in the supermatrices) and therefore less strong model misspecification. It should be noted, that there is no general pattern concerning how the species-specific  $|z|$  scores changed across matrix manipulations. Nevertheless, our approach to also remove sites with unique amino acids in the two species of Pararotatoria resulted in reduced  $|z|$  scores concerning the amino-acid compositional deviation of each of these two species. Lastly, *Brachionus calyciflorus*, *H. microstoma*, and *L. mae-rski* consistently showed much higher  $|z|$  scores in comparison with other species in the datasets.

#### Evaluation of four phylogenetic hypotheses of Syndermata in concatenation-based analyses

We summarized the properties of supermatrices that supported (or not) the four selected phylogenetic hypotheses of Syndermata (see Fig. 3a–3d). The Seisonidea-sister hypothesis (Seisonidea as sister to a clade Acanthocephala+Bdelloidea+Monogononta) was inferred by the vast majority of supermatrices under the profile mixture models before removing sites with unique amino acids for *P. laevis* and *S. nebaliae* (10 out of 14 supermatrices). However, we observed that supermatrices whose analyses did not result in the inference of the Seisonidea-sister hypothesis were characterized by lower standard deviation of LB scores (median inferred=27.65, median not inferred=26.74), higher TORCV values (median inferred=0.86, median not inferred=1.54), and higher saturation scores (median inferred=0.58, median not inferred=0.78, Fig. 3a–3d, Online Resource 1: Figs: S141, S142). The same pattern concerning these three properties is observed for the datasets whose analyses supported the Lemniscea hypothesis (Fig. 4b, Online Resource 1: Figs. S141, S142). In summary, these two hypotheses were inferred under dataset and species-tree properties that



are known to increase the possibility of systematic errors (Fig. 3a, 3b).

In contrast, supermatrices and their inferred species trees that supported the Hemirotrifera or Pararotatoria hypothesis had on average more desirable properties than supermatrices and corresponding species trees that did not support these two hypotheses (Fig. 3c, 3d). Specifically, datasets that supported the Hemirotrifera hypothesis were characterized by lower standard deviation of LB scores (median inferred=26.54, median not inferred=27.51), higher TORCV values (median inferred=1.61, median not inferred=1.09), and higher saturation scores (median inferred=0.80, median not inferred=0.65) than the datasets that did not result in the inference of Hemirotrifera (Fig. 3c, Online Resource 1: Figs. S141, S142). In a similar fashion, supermatrices whose analyses resulted in the inference of Pararotatoria were characterized by better values for the above-mentioned dataset- and species-tree properties than supermatrices whose analyses did not support the

Pararotatoria hypothesis (Fig. 3d, see also Online Resource 1: Figs. S141–S148). Overall, the Hemirotrifera and Pararotatoria hypotheses were therefore supported under dataset and species-tree conditions that are less likely to cause systematic errors.

#### Species-tree inference of syndermatan relationships from multi-copy orthogroups

All but one species-tree analyses using a combination of single- and multi-copy OGs, and all species present (no. of species=12), supported the Syndermata hypothesis (topology 3, Fig. 5, datasets A–F). Specifically, the SpeciesRax analysis did not result in a clade of Acanthocephala + Bdelloidea + Monogononta + Seisonidea when we used the default gene trees of Orthofinder for species-tree inference (topology 1, dataset A, Fig. 5). However, when we selected the best-fit models in ModelFinder and recalculated the individual gene trees, we were able to infer syndermatan monophyly irrespective of the species-tree method (Fig. 5, datasets

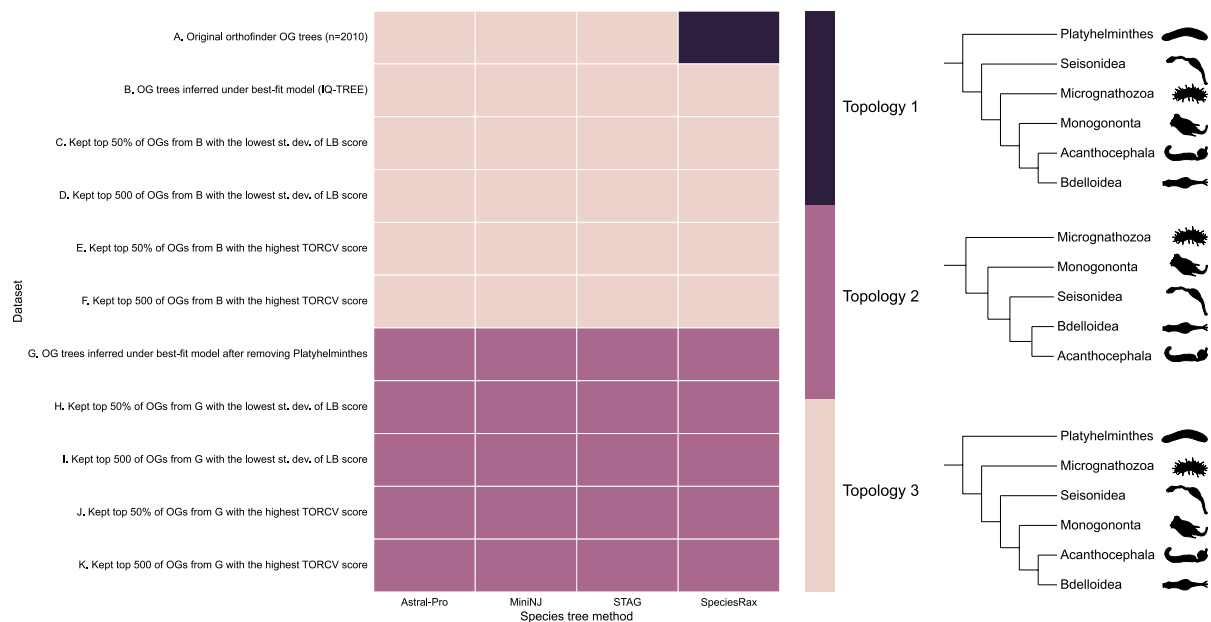


**Fig. 5** Results of gene-tree-based phylogenetic analyses of Syndermata depending on the dataset and species-tree method used. Rows in the grid correspond to different subsets of orthogroups and their inferred gene trees. Colors show the different topologies obtained depending on the species-tree method applied (different columns represent different species-tree inference methods). Dataset A consists of all the gene trees

that were inferred automatically by Orthofinder ( $n=2,010$ ). Datasets A–F correspond to orthogroup multiple sequence alignments and their inferred trees by including sequences of Platyhelminthes. Datasets G–K correspond to sets of orthogroups and gene trees that were inferred after the two species of Platyhelminthes were removed from the multiple sequence alignments



B–F). All species-tree analyses of datasets that included Platyhelminthes (B–F) suggested Seisonidea as sister to all remaining syndermatan lineages (i.e., Acanthocephala, Bdelloidea, Monogononta). This result was stable irrespective of the number of OGs analyzed (see datasets B–F, Fig. 5). We observed, however, that the inferred phylogenetic relationships of Syndermata were dependent on the set of species in the initial OGs. More specifically, we repeated all species-tree analyses after removing all sequences of Platyhelminthes from the individual OGs. The results show that when sequences of Platyhelminthes were not part of the individual MSAs of OGs, then Monogononta emerged as sister to an Acanthocephala + Bdelloidea + Seisonidea clade (the Hemirotofera hypothesis, topology

2, Fig. 5). A clade of Acanthocephala + Seisonidea (the Pararotatoria hypothesis) was not inferred in any of our species-tree analyses that combined information from single- and multi-copy OGs (Fig. 5).

#### Microsynteny-based phylogenetic reconstruction of syndermatan relationships

The total number of characters (i.e., synteny clusters) used to construct the phylogeny of Syndermata differed slightly depending on the parameters applied for syntenic block detection ( $n=17,703$ ,  $n=17,711$  and  $n=17,571$ ; see Figs. 6a, 6b and Online Resource 1: Fig. S149, respectively). We observed that the majority of microsynteny clusters were specific to bdelloid rotifers,

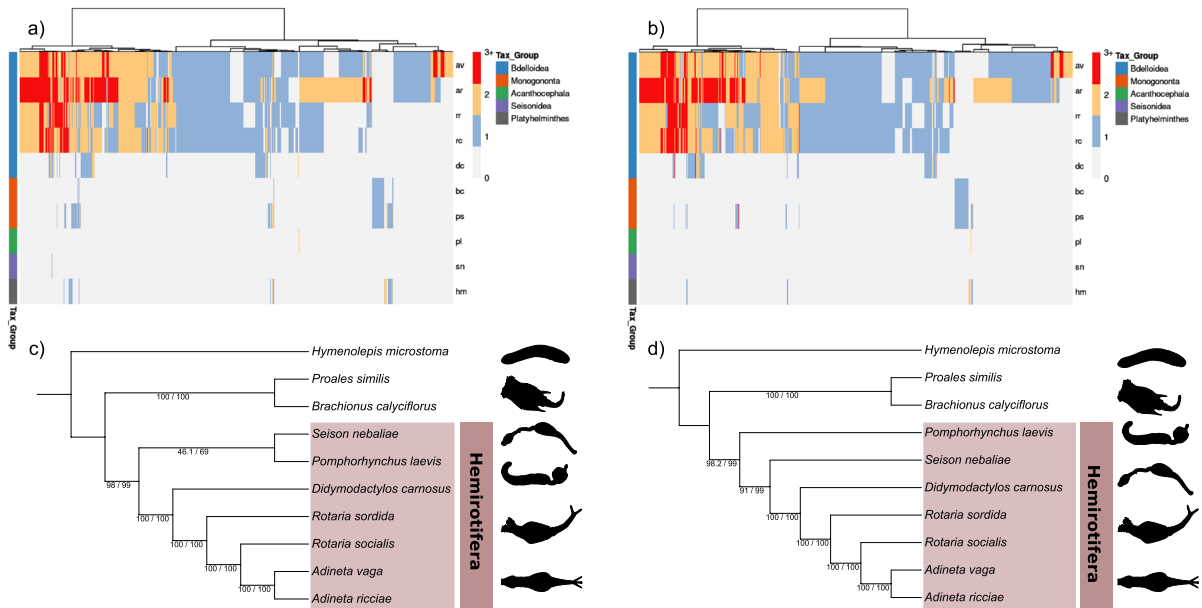


**Fig. 6** Results of microsynteny-based phylogenomic profiling and phylogenetic reconstructions of Syndermata. **a** Phylogenomic profiling of synteny clusters across syndermatan genomes when using the parameters: anchors=2 and max\_gaps=60 for syntenic block definition; **b** phylogenomic profiling of syntenic clusters across syndermatan genomes when using the parameters: anchors=3 and max\_gaps=60 for syntenic block definition. Columns in the heatmaps correspond to different syntenic clusters that are present or absent in different species. Each syntenic cluster (i.e., character) corresponds to a set of anchored genes within a syntenic block across species. Colors show the number of genes per cluster for each species (0, 1, 2 or  $\geq 3$ ). Multiple genes for a species in a cluster could be due to uncollapsed haplotypes or polyploidization. Initials in the rows of the heatmaps correspond to the species names

(av: *Adineta vaga*, ar: *Adineta ricciae*, rr: *Rotaria sordida*, rc: *Rotaria socialis*, dc: *Didymodactylos carnosus*, bc: *Brachionus calyciflorus*, ps: *Proales similis*, pl: *Pomphorhynchus laevis*, sn: *Seison nebaliae*, hm: *Hymenolepis microstoma*); **c** Cladogram showing the inferred phylogenetic relationships of Syndermata when using the parameters anchors=2 and max\_gaps=60 for syntenic block definition; **d** Cladogram showing the inferred phylogenetic relationships of Syndermata when using the parameters anchors=3 and max\_gaps=60 for syntenic block definition. Since some internal branches were very short, only the topology of the inferred species trees is depicted. Statistical branch support of the inferred trees is shown based on 2,000 SH-aLRT and 1,000 ultrafast bootstrap (UFB) replicates (SH-aLRT / UFB)

showing a drastic reduction of synteny conservation across syndermatan genomes (see Figs. 6a, 6b). *Schmidtea mediterranea* was automatically excluded from the phylogenomic profiles constructed by syntenet, potentially due to the lack of synteny to other genome assemblies in the dataset (see Fig. 6a, 6b, Online Resource 1: Fig. S149). The MK+FQ+ASC+R2 model was selected as best-fit model for all different matrices of binary characters irrespective of the parameters used for synteny block definition. Phylogenetic trees inferred from the binary-data matrices suggested Monogononta as sister to a clade Acanthocephala+Bdelloidea+Seisonidea (i.e., the Hemirotifera hypothesis). The Hemirotifera received strong branch support in all analyses (e.g., Fig. 6c: 99% UFB and 98% SH-aLRT) irrespective of the parameters used for syntenic block detection (Figs. 6c, 6d, Online Resource 1: Fig. S150). Despite this, the phylogenetic relationships among Acanthocephala, Bdelloidea, and Seisonidea differed across analyses with different synteny-block parameters (Figs. 6c, 6d, Online Resource 1: Fig. S150). Only one phylogenetic analysis supported the Pararotatoria hypothesis within Hemirotifera (Fig. 6a, parameters: anchors=2 and max\_gaps=60), in agreement with the results of our concatenation-based analysis of supermatrix H (Fig. 4), but this relationship was poorly supported in the phylogenetic analyses of microsynteny data (46.1% SH-aLRT and 69% UFB support, Fig. 6a).

We inferred site-concordance factors (SCF, SCFL) to quantify the strength of the microsynteny signal in favor of the Monogononta-sister and the Seisonidea-sister hypotheses. For five out of six site-concordance factor analyses, the Monogononta-sister (i.e., Hemirotifera) hypothesis was supported by higher site-concordance factor scores than the Seisonidea-sister hypothesis (i.e., Bdelloidea+Monogononta+Acanthocephala, see Online Resource 1: Fig. S151). Furthermore, maximum-likelihood-based SCFL scores, which are less prone to homoplasy errors than parsimony-based SCF scores (Kück et al., 2022; Mo et al., 2023), showed significantly higher values in support of Hemirotifera than for a clade Bdelloidea+Monogononta+Acanthocephala across all microsynteny parameters (Monogononta-sister or Hemirotifera hypothesis: 44.5%, 99.5% and 97.5%; Seisonidea-sister or Bdelloidea+Monogononta+Acanthocephala hypothesis: 0.35%, 0.35% and 2.26%, respectively; Online Resource 1: Fig. S151).

## Discussion

Seeking congruence across analyses concerning the phylogenetic relationships of Syndermata

Our study demonstrates the power of combining several sources of evidence to address challenging phylogenetic questions, such as sequence-based phylogenomics (concatenation- and gene tree-based) and gene colinearity (here referred to as microsynteny conservation; Simakov et al., 2022). Such integrative approaches have received increased attention in the last decade (Niehuis et al., 2012; Sielaff et al., 2016; Cloutier et al., 2019; Drillon et al., 2020; Ontano et al., 2021; Zhao et al., 2021; Parey et al., 2023). The results of our independent phylogenetic approaches enable us to establish the Hemirotifera hypothesis (i.e., Monogononta-sister hypothesis) as the most plausible scenario of early syndermatan evolution. Specifically, we show that a clade Acanthocephala+Bdelloidea+Seisonidea is inferred by the analyses of supermatrices with desirable properties but is also supported by microsynteny-based phylogenetic reconstructions and by species-tree methods that use multi-copy OGs. Furthermore, we show that a clade Acanthocephala+Seisonidea (Pararotatoria) is supported by the analyses of supermatrices with desirable properties and partially also by microsynteny-based phylogenetic analyses. However, species-tree methods that rely on multi- and single-copy orthogroups only supported Hemirotifera when distantly related species of Platyhelminthes had previously been removed from the OGs (Fig. 5). The use of distantly related outgroups is a well-known source of error in phylogenetic reconstructions. This is because distantly related species might be characterized by the differences in the evolutionary rates and amino-acid sequence composition, resulting in their artefactual grouping with lineages of the ingroup (Philippe & Laurent, 1998; Li et al., 2012; Pisani et al., 2015; Borowiec et al., 2019). In our analyses, there is a considerable phylogenetic distance between Platyhelminthes and the species of Micrognathozoa+Syndermata (Laumer et al., 2019; Marlétaz et al., 2019), which most likely negatively affected our phylogenetic reconstructions. This is particularly evident in most concatenation-based analyses with the site-homogeneous LG+F+R5 model that did not support the Syndermata hypothesis when Platyhelminthes

were included in the analyses (Fig. 2c). Our observations of the negative effects of using a distantly related outgroup are in agreement with similar observations in previous phylogenomic analyses of syndermatan relationships (e.g., Mauer et al., 2021).

Moreover, our results illustrate the sensitivity of both gene tree-based and concatenation-based species-tree methods to outgroup selection, potentially due to long-branch attraction, or more generally model misspecification (Roch & Warnow, 2015; Roch et al., 2019; see also Vasilikopoulos et al., 2019). Overall, we suggest that the use of a distantly related outgroup without comprehensive sampling of the intermediate outgroup lineages should be avoided, if possible, in future sequence-based phylogenomic studies. On the other hand, genome structural approaches might be less prone to phylogenetic artifacts (see for example Sielaff et al., 2016). Additional whole-genome data from closely related gnathiferan groups (e.g., Micrognathozoa and Gnathostomulida) might facilitate more direct tests of this hypothesis. Indeed, a more comprehensive sampling of outgroup species but only from closely related lineages of Gnathifera, such as Micrognathozoa, Gnathostomulida, and Chaetognatha might be beneficial for inferring the internal phylogeny of Syndermata in future sequence-based analyses (see, e.g., Wey-Fabrizius et al., 2014). The addition of genomic data from other species of Acanthocephala and Seisonidea might also be beneficial. However, as pointed out by other authors, an increased sampling of closely related outgroup species might not solve the problem completely, as some of these closely related outgroup species might be characterized by compositional and other heterogeneities that could then affect the topology of the ingroup (Borowiec et al., 2019). An acceptable solution would then be to choose a good sampling of only closely related outgroup lineages that also have desirable properties such as low heterogeneity of sequence composition and evolutionary rates in relation to the ingroup taxa.

Our evaluation of the properties of supermatrices and their inferred trees that supported the Hemirotifera and Pararotatoria hypotheses provides evidence that the inference of these clades is likely not due to systematic error. On the contrary, supermatrices and inferred trees that do not support the Hemirotifera and Pararotatoria hypotheses seem to have properties that are associated with increased possibility of systematic

error, such as increased levels of branch-length heterogeneity (Struck, 2014; Struck et al., 2014; Kapli et al., 2021). In fact, we observed improved dataset and tree characteristics upon removal of sites reflecting lineage-specific acceleration of sequence evolution in Acanthocephala and Seisonidea and, at the same time, an increased proportion of analyses that supported Hemirotifera and Pararotatoria. The Pararotatoria hypothesis is also strongly supported by analyses of morphological data providing further evidence to support our preferred hypotheses from concatenation-based analyses (Fig. 4; Ahlrichs, 1997, 1998; Zrzavý, 2001). In contrast to the Hemirotifera hypothesis, however, the microsynteny-based phylogenomic analyses only partially supported the monophyly of Acanthocephala + Seisonidea, as only one of three analyses resulted in the inference of this clade with very low branch support (Fig. 6c). We observed, however, very few informative synteny clusters for inferring the deep phylogeny of Syndermata. Currently, we cannot conclude if this is due to the low quality of the analyzed genomes or more generally due to the low degree of conserved gene colinearity across genomes of Syndermata (Fig. 6). Since most genomes included in our analyses were based on short-read sequencing technologies and therefore had low degree of contiguity, this question will be answered once highly complete and contiguous genomes from all clades of Syndermata and outgroups become available. The first chromosome-level assembly of a bdelloid rotifer is a promising step in this direction (Simion et al., 2021).

The Pararotatoria hypothesis was not supported by our species-tree analyses of multi-copy OGs (Fig. 5). Despite this, it is generally accepted that there are many challenges when inferring gene trees at deep evolutionary timescales. Specifically, it is challenging to disentangle biological gene-tree heterogeneity from gene-tree estimation error due to low phylogenetic signal or even systematic error (Roch & Warnow, 2015; Springer & Gatesy, 2016; Bryant & Hahn, 2020; Simion et al., 2020; Vasilikopoulos et al., 2021a). Irrespective of the source of gene-tree errors at deep evolutionary timescales, these errors might affect the accuracy of the corresponding species-tree methods (Roch & Warnow, 2015; Springer & Gatesy, 2016; Roch et al., 2019). Thus, it is possible that our gene-tree-based methods failed to recover Acanthocephala and Seisonidea as sister groups due

to gene-tree estimation errors as a result of either low phylogenetic signal or systematic error. The latter hypothesis is supported by the observation that removal of sequences of Platyhelminthes from the MSAs of individual OGs altered the internal topology of Syndermata for these species-tree methods, from a Seisonidea-sister to a Monogononta-sister (i.e., Hemirotifera) hypothesis, similarly to some results from the concatenation-based analyses. Therefore, both the Hemirotifera and Pararotatoria hypotheses remain plausible hypotheses of syndermatan evolution but should be both further corroborated once highly complete and contiguous syndermatan genomes become available.

Our comprehensive phylogenomic analyses using data- and tree-evaluation approaches identify some phylogenetic hypotheses of syndermatan relationships as less likely than others. For example, the Seisonidea-sister and Lemniscea hypotheses are less well supported by our results as they are not inferred from our microsynteny-based phylogenetic reconstructions. Additionally, statistical branch support for a clade of Acanthocephala + Bdelloidea + Monogononta is reduced when selecting the most reliable genes for concatenated analysis, and it disappears in the absence of a distantly related outgroup in some sequence-based analyses (concatenation- or gene-tree-based). Moreover, further evaluation of the properties of the supermatrices and trees that supported these two hypotheses (Seisonidea-sister and Lemniscea) suggested that they are inferred under dataset and species-tree properties typically associated with systematic errors (Figs. 3a and 3b). Hence, these latter two hypotheses are not widely supported from the analyses of different types of data, tree reconstruction, and data-evaluation methods. Although we cannot rule out these two hypotheses completely, especially given that they were derived in the majority of sequence-based analyses, we consider them as less likely based on our results. Furthermore, our observation that the Lemniscea and Seisonidea-sister hypotheses were inferred under conditions with elevated possibility of systematic error, despite being the most frequently inferred hypotheses in sequence-based analyses, suggests that the consensus to species phylogenies should ideally rely on methodologically diverse approaches and different types of data, including morphology and genome structures, rather than exclusively on sequence-based analyses. It should be

noted, however, that except for Pararotatoria, none of the other three hypotheses that we evaluated receives strong support from morphology so far, a phenomenon that is relatively common in molecular systematics (Pisani et al., 2007). This underlines the importance of critical assessment of the results of both molecular and morphological studies for resolving these conflicts through the process of reciprocal illumination (e.g., Ragsdale & Baldwin, 2010; Gustafson et al., 2021; Sharma et al., 2021).

Implications for the evolution of morphological characters, reproductive modes, and parasitic lifestyles within Syndermata

A clade of Acanthocephala + Seisonidea (Pararotatoria) as sister to Bdelloidea is consistent with prevalent views concerning the evolution of endoparasitism within Syndermata (Herlyn, 2021). Specifically, it is currently hypothesized that the endoparasitic lifestyle of Acanthocephala evolved via an intermediate epibiotic (i.e., epizoic) stage on jawed arthropods, such as the one observed in species of the genus *Seison* (Seisonidea). This hypothesis states that there has been a transition from a free-living lifestyle in the common ancestor of Syndermata to an epizoic (or even ectoparasitic, Ricci et al., 1993) lifestyle in the stem lineage of Pararotatoria and a subsequent transition to an endoparasitic lifestyle in the stem lineage of Acanthocephala (and also the addition of a definite gnathostome host in Acanthocephala; Herlyn et al., 2003; Wey-Fabrizius et al., 2014; Sielaff et al., 2016; Herlyn, 2021).

Another important result of our study is that the Eurotatoria hypothesis (i.e., that Bdelloidea and Monogononta are sister groups) seems unlikely, as it was recovered in the analyses of only two supermatrices, but only one of these was using a site-heterogeneous model. This result is congruent with most molecular studies to date (e.g., Garey et al., 1996, 1998; Witek et al., 2008). Similarly to previous hypotheses for the evolution of endoparasitism in Acanthocephala via an intermediate epizoic stage (Herlyn et al., 2003; Herlyn, 2021), one could hypothesize a transition from sexual reproduction to obligate asexuality through an intermediate stage of facultative sexual reproduction within Syndermata, as has been suggested in other organisms (Larose et al., 2023). If Bdelloidea and Monogononta were indeed

sister groups, a plausible explanation for the evolution of reproductive modes within Syndermata would be that there was a transition from sexual reproduction in the common ancestor of Syndermata to facultative sexual reproduction in the stem lineage of Eurotatoria and subsequent complete loss of sex in Bdelloidea. This could also be supported by the conditional presence of non-canonical meiosis in Bdelloidea and Monogononta that would then represent the ancestral state of Eurotatoria (Terwagne et al., 2022). However, our results show that such a hypothesis is unlikely, as do most molecular studies to date (e.g., Witek et al., 2008; Wey-Fabrizius et al., 2014; Sielaff et al., 2016; Mauer et al., 2021). Consequently, an evolutionarily independent modification of the meiotic machinery in Bdelloidea and in Monogononta resulting in obligate or facultative asexuality is more likely following the phylogenomic results presented here. However, it should be emphasized that the hypothesis of an independent evolution of a non-canonical meiosis in Bdelloidea and Monogononta depends on whether this modified meiosis is indeed present in all species of Bdelloidea and Monogononta. Until now, there has been only one detailed cytological study of oogenesis in one bdelloid species (*Adineta vaga*) and a reinterpretation of old cytological results from one monogonont species (Terwagne et al., 2022). Further cytological studies of more species of Monogononta and Bdelloidea could provide additional tests of these hypotheses. Sexual reproduction with separate sexes is probably the ancestral state of Syndermata, since there is no evidence that sexual reproduction can be regained once it is lost. Sexual reproduction with separate sexes in the common ancestor of Syndermata is supported by the presence of males and females in all syndermatan groups except Bdelloidea, but the evolutionary sequence of events among different reproductive modes within Syndermata remains a mystery.

Our hypothesis on the evolution of reproductive modes within Syndermata also depends on the reproductive mode of their closest outgroup; the Micrognathozoa. However, to our knowledge, clear evidence for the reproductive mode of *L. maerski* is not currently available. To date, only evidence of females can be considered reliable, suggesting that Micrognathozoa reproduce parthenogenetically (Kristensen & Funch, 2000). Despite this, there is also evidence of sculptured eggs besides smooth-shelled eggs, so sexual reproduction could also occur (De Smet,

2002). Moreover, young stages of *L. maerski* reportedly exhibit paired refractive bodies which could represent testicles, suggesting that *L. maerski* might be a protandrous hermaphrodite (Sørensen & Kristensen, 2015). Therefore, although males have not been conclusively demonstrated, the above-described features suggest that the presence of males, either as separate or protandrous individuals, cannot be excluded. In-depth studies on the reproductive mode of Micrognathozoa will facilitate formulating more detailed hypotheses on the evolution of reproductive modes within Syndermata.

The Hemirotifera and Pararotatoria hypotheses also necessitate a reevaluation of the evolution of several morphological and ecological characters within Syndermata. For example, characters such as the ciliated corona of Bdelloidea and Monogononta may represent the ancestral state of Syndermata with secondary modification in the stem lineage of Pararotatoria. In fact, locomotory ciliation is present in other groups of Gnathifera, such as Micrognathozoa and Gnathostomulida, but the cilia cover larger regions of the body in these groups than in Bdelloidea and Monogononta (Sterrer, 1972; Kristensen & Funch, 2000; Bekkouche & Worsaae, 2016; Sørensen et al., 2016). In contrast to Bdelloidea and Monogononta, Seisonidea have a reduced corona with minimal ciliation and Acanthocephala lack ciliation altogether (Ricci et al., 1993; Mark Welch, 2000). Therefore, there is likely a trend for reduction of locomotory ciliation within Pararotatoria, from the ciliated corona in the common syndermatan ancestor to the partial and complete loss of ciliation in Seisonidea and Acanthocephala, respectively. These features are probably secondary modifications connected to the epizoic or endoparasitic lifestyle of Seisonidea and Acanthocephala. The need for the reinterpretation of morphological evolution might apply to additional characters that are considered synapomorphies of Rotifera sensu stricto such as the presence of a muscular pharynx (i.e., mastax) that is specialized and unique in Seisonidea (Ricci et al., 1993; Segers & Melone, 1998), while according to current knowledge is absent in Acanthocephala (Mark Welch, 2000). Moreover, species belonging to the sister group of Syndermata, the Micrognathozoa, possess a muscular pharynx with hard pieces that are very similar to rotifer trophi, and are even more complex than those of rotifers (Kristensen & Funch, 2000; De Smet, 2002; Sørensen,



2003). Thus, it is not unlikely that the typical mastax as it is known from Monogononta and Bdelloidea was present in the common ancestor of Syndermata with subsequent secondary modifications in species of Parrotatoria, as a result of their epizoic or endoparasitic lifestyle.

**Acknowledgements** We thank all members of the Research Unit of Molecular Biology and Evolution (Université libre de Bruxelles, Belgium) and the participants of the XVI International Rotifer Symposium for the interesting and helpful discussions. This work was funded by the Philippe WIENER – Maurice ANSPACH Foundation through a collaborative project of KVD and TGB. This research was also supported by the grant agreement 725998 (RHEA) from the European Research Council (ERC CoG) to KVD, providing funding for AV. RWN, CGW, and TGB were funded by Natural Environment Research Council grants NE/M01651X/1 and NE/S010866/1. Financial support by the Deutsche Forschungsgemeinschaft (HE3487/5-1) to HH is gratefully acknowledged.

**Data availability** The datasets supporting the conclusions of this article are available in the figshare digital repository (<https://doi.org/10.6084/m9.figshare.22182697.v1>). Custom bioinformatic scripts that were used for data processing are also provided on github ([https://github.com/alexvasilikop/Rotifer\\_phylogeny](https://github.com/alexvasilikop/Rotifer_phylogeny)).

#### Declarations

**Competing interests** The authors declare that they have no competing interests.

#### References

- Ababneh, F., L. S. Jermiin, C. Ma & J. Robinson, 2006. Matched-pairs tests of homogeneity with applications to homologous nucleotide sequences. *Bioinformatics* 22: 1225–1231. <https://doi.org/10.1093/bioinformatics/btl064>.
- Ahlrichs, W. H., 1995. Ultrastruktur und Phylogenie von *Seison nebaliae* (Grube 1859) und *Seison annulatus* (Claus 1876). Hypothesen zu phylogenetischen Verwandtschaftsverhältnissen innerhalb der Bilateria. Cuvilier, Göttingen.
- Ahlrichs, W. H., 1997. Epidermal ultrastructure of *Seison nebaliae* and *Seison annulatus*, and a comparison of epidermal structures within the Gnathifera. *Zoomorphology* 117: 41–48. <https://doi.org/10.1007/s004350050028>.
- Ahlrichs, W. H., 1998. Spermatogenesis and ultrastructure of the spermatozoa of *Seison nebaliae* (Syndermata). *Zoomorphology* 118: 255–261. <https://doi.org/10.1007/s004350050074>.
- Almeida-Silva, F., T. Zhao, K. K. Ullrich, M. E. Schranz & Y. Van de Peer, 2023. Syntenet: an R/Bioconductor package for the inference and analysis of synteny networks. *Bioinformatics* 39: btac806. <https://doi.org/10.1093/bioinformatics/btac806>.
- Bekkouche, N. & L. Gąsiorowski, 2022. Careful amendment of morphological data sets improves phylogenetic frameworks: re-evaluating placement of the fossil *Amiskwia sagittiformis*. *Journal of Systematic Palaeontology* 20: 2109217. <https://doi.org/10.1080/14772019.2022.2109217>.
- Bekkouche, N. & K. Worsaae, 2016. Nervous system and ciliary structures of Micrognathozoa (Gnathifera): evolutionary insight from an early branch in Spiralia. *Royal Society Open Science* 3: 160289. <https://doi.org/10.1098/rsos.160289>.
- Bollback, J. P., 2002. Bayesian model adequacy and choice in phylogenetics. *Molecular Biology and Evolution* 19: 1171–1180. <https://doi.org/10.1093/oxfordjournals.molbev.a004175>.
- Borowiec, M. L., C. Rabeling, S. G. Brady, B. L. Fisher, T. R. Schultz & P. S. Ward, 2019. Compositional heterogeneity and outgroup choice influence the internal phylogeny of the ants. *Molecular Phylogenetics and Evolution* 134: 111–121. <https://doi.org/10.1016/j.ympev.2019.01.024>.
- Bowker, A. H., 1948. A test for symmetry in contingency tables. *Journal of the American Statistical Association* 43: 572–574. <https://doi.org/10.2307/2280710>.
- Bradley, R. K., A. Roberts, M. Smoot, S. Juvekar, J. Do, C. Dewey, I. Holmes & L. Pachter, 2009. Fast statistical alignment. *PLoS Computational Biology* 5: e1000392. <https://doi.org/10.1371/journal.pcbi.1000392>.
- Bryant, D., & M. W. Hahn, 2020. The concatenation question. In Scornavacca, C., F. Delsuc, & N. Galtier (eds), *Phylogenetics in the genomic era*. No commercial publisher | Authors' open access book: 3.4:1–3.4:23. <https://hal.science/hal-02535651>.
- Buchfink, B., K. Reuter & H.-G. Drost, 2021. Sensitive protein alignments at tree-of-life scale using DIAMOND. *Nature Methods* 18: 366–368. <https://doi.org/10.1038/s41592-021-01101-x>.
- Clément, P., 1993. The phylogeny of rotifers: molecular, ultrastructural and behavioural data. *Hydrobiologia* 255: 527–544. <https://doi.org/10.1007/BF00025882>.
- Cloutier, A., T. B. Sackton, P. Grayson, M. Clamp, A. J. Baker & S. V. Edwards, 2019. Whole-genome analyses resolve the phylogeny of flightless birds (Palaeognathae) in the presence of an empirical anomaly zone. *Systematic Biology* 68: 937–955. <https://doi.org/10.1093/sysbio/syz019>.
- Crisuolo, A. & S. Gribaldo, 2010. BMGE (Block Mapping and Gathering with Entropy): a new software for selection of phylogenetic informative regions from multiple sequence alignments. *BMC Evolutionary Biology* 10: 210. <https://doi.org/10.1186/1471-2148-10-210>.
- Dell’Ampio, E., Meusemann, K., Szucsich, N. U., Peters, R. S., Meyer, B., Borner, J., et al, 2014. Decisive data sets in phylogenomics: lessons from studies on the phylogenetic relationships of primarily wingless insects. *Molecular Biology and Evolution*, 31, 239–249. <https://doi.org/10.1093/molbev/mst196>.
- De Smet, W. H., 2002. A new record of *Limmognathia mae-rski* Kristensen & Funch, 2000 (Micrognathozoa) from the subantarctic Crozet Islands, with redescription of the



- troph. *Journal of Zoology* 258: 381–393. <https://doi.org/10.1017/S095283690200153X>.
- Di Franco, A., R. Poujol, D. Baurain & H. Philippe, 2019. Evaluating the usefulness of alignment filtering methods to reduce the impact of errors on evolutionary inferences. *BMC Evolutionary Biology* 19: 21. <https://doi.org/10.1186/s12862-019-1350-2>.
- Drillon, G., R. Champeimont, F. Oteri, G. Fischer & A. Carbone, 2020. Phylogenetic reconstruction based on synteny block and gene adjacencies. *Molecular Biology and Evolution* 37: 2747–2762. <https://doi.org/10.1093/molbev/msaa114>.
- Emms, D. M., & S. Kelly, 2018. STAG: species tree inference from all genes. *BioRxiv* 267914. <https://doi.org/10.1101/267914>.
- Emms, D. M. & S. Kelly, 2019. OrthoFinder: phylogenetic orthology inference for comparative genomics. *Genome Biology* 20: 238. <https://doi.org/10.1186/s13059-019-1832-y>.
- Ferraguti, M. & G. Melone, 1999. Spermiogenesis in *Seison nebaliae* (Rotifera, Seisonidea): further evidence of a rotifer-acanthocephalan relationship. *Tissue and Cell* 31: 428–440. <https://doi.org/10.1054/tice.1999.0012>.
- Feuda, R., M. Dohrmann, W. Pett, H. Philippe, O. Rota-Stabelli, N. Lartillot, G. Wörheide & D. Pisani, 2017. Improved modeling of compositional heterogeneity supports sponges as sister to all other animals. *Current Biology* 27: 3864–3870. <https://doi.org/10.1016/j.cub.2017.11.008>.
- Fontaneto, D., 2014. Molecular phylogenies as a tool to understand diversity in rotifers. *International Review of Hydrobiology* 99: 178–187. <https://doi.org/10.1002/iroh.201301719>.
- Fontaneto, D. & W. H. De Smet, 2015. Rotifera. In Schmidt-Rhaesa, A. (ed), *Handbook of Zoology*, Vol. 3. De Gruyter, Berlin: 217–300. *Gastrotricha and Gnathifera*.
- Fontaneto, D. & U. Jondelius, 2011. Broad taxonomic sampling of mitochondrial cytochrome c oxidase subunit I does not solve the relationships between Rotifera and Acanthocephala. *Zoologischer Anzeiger* 250: 80–85. <https://doi.org/10.1016/j.jcz.2010.11.005>.
- Funch, P., M. V. Sørensen & M. Obst, 2005. On the phylogenetic position of Rotifera – have we come any further? *Hydrobiologia* 546: 11–28. <https://doi.org/10.1007/s10750-005-4093-6>.
- Fussmann, G. F., 2011. Rotifers: excellent subjects for the study of macro- and microevolutionary change. *Hydrobiologia* 662: 11–18. <https://doi.org/10.1007/s10750-010-0515-1>.
- García-Varela, M. & S. A. Nadler, 2006. Phylogenetic relationships among Syndermata inferred from nuclear and mitochondrial gene sequences. *Molecular Phylogenetics and Evolution* 40: 61–72. <https://doi.org/10.1016/j.ympev.2006.02.010>.
- Garey, J. R., T. J. Near, M. R. Nonnemacher & S. A. Nadler, 1996. Molecular evidence for Acanthocephala as a subtaxon of Rotifera. *Journal of Molecular Evolution* 43: 287–292. <https://doi.org/10.1007/BF02338837>.
- Garey, J. R., A. Schmidt-Rhaesa, T. J. Near & S. A. Nadler, 1998. The evolutionary relationships of rotifers and acanthocephalans. *Hydrobiologia* 387: 83–91. <https://doi.org/10.1023/A:1017060902909>.
- Grabherr, M. G., B. J. Haas, M. Yassour, J. Z. Levin, D. A. Thompson, I. Amit, X. Adiconis, L. Fan, R. Raychowdhury, Q. Zeng, Z. Chen, E. Muceli, N. Hacohen, A. Gnirke, N. Rhind, F. Di Palma, B. W. Birren, C. Nusbaum, K. Lindblad-Toh, N. Friedman & A. Regev, 2011. Full-length transcriptome assembly from RNA-Seq data without a reference genome. *Nature Biotechnology* 29: 644–652. <https://doi.org/10.1038/nbt.1883>.
- Guindon, S., J. F. Dufayard, V. Lefort, M. Anisimova, W. Hordijk & O. Gascuel, 2010. New algorithms and methods to estimate maximum-likelihood phylogenies: assessing the performance of PhyML 3.0. *Systematic Biology* 59: 307–321. <https://doi.org/10.1093/sysbio/syq010>.
- Gustafson, G. T., K. B. Miller, M. C. Michat, Y. Alarie, S. M. Baca, M. Balke, & A. E. Z. Short, 2021. The enduring value of reciprocal illumination in the era of insect phylogenomics: a response to Cai et al. (2020). *Systematic Entomology* 46: 473–486. <https://doi.org/10.1111/syen.12471>.
- Hankeln, T., A. R. Wey-Fabrizius, H. Herlyn, M. Weber, M. P. Nesnidal, T. H. Struck, & A. Witek, 2014. Phylogeny of platyzoan taxa based on molecular data In Wägele, J. W., & T. Bartolomaeus (eds), *Deep metazoan phylogeny: the backbone of the tree of life*. De Gruyter: 105–126.
- Herlyn, H., 2021. Thorny-headed worms (Acanthocephala): jaw-less members of jaw-bearing worms that parasitize jawed arthropods and jawed vertebrates. In De Baets, K. & J. W. Huntley (eds), *The Evolution and Fossil Record of Parasitism*, Topics in Geobiology, Vol. 49. Springer, Cham: 273–313.
- Herlyn, H., O. Piskurek, J. Schmitz, U. Ehlers & H. Zischler, 2003. The syndermatan phylogeny and the evolution of acanthocephalan endoparasitism as inferred from 18S rDNA sequences. *Molecular Phylogenetics and Evolution* 26: 155–164. [https://doi.org/10.1016/S1055-7903\(02\)00309-3](https://doi.org/10.1016/S1055-7903(02)00309-3).
- Hoang, D. T., O. Chernomor, A. von Haeseler, B. Q. Minh & S. V. Le, 2018. UFBoot2: improving the ultrafast bootstrap approximation. *Molecular Biology and Evolution* 35: 518–522. <https://doi.org/10.1093/molbev/msx281>.
- Howe, K. L., B. J. Bolt, M. Shafie, P. Kersey & M. Berriman, 2017. WormBase ParaSite – a comprehensive resource for helminth genomics. *Molecular and Biochemical Parasitology* 215: 2–10. <https://doi.org/10.1016/j.molbiopara.2016.11.005>.
- Huerta-Cepas, J., F. Serra & P. Bork, 2016. ETE 3: reconstruction, analysis, and visualization of phylogenomic data. *Molecular Biology and Evolution* 33: 1635–1638. <https://doi.org/10.1093/molbev/msw046>.
- Hunter, J. D., 2007. Matplotlib: a 2D graphics environment. *Computing in Science & Engineering* 9: 90–95. <https://doi.org/10.1109/MCSE.2007.55>.
- Hur, J. H., K. Van Doninck, M. L. Mandigo & M. Meselson, 2009. Degenerate tetraploidy was established before bdelloid rotifer families diverged. *Molecular Biology and Evolution* 26: 375–383. <https://doi.org/10.1093/molbev/msn260>.
- Jermiin, L. S., V. Jayaswal, F. Ababneh, & J. Robinson, 2008. Phylogenetic model evaluation In Keith, J. M. (ed), *Bioinformatics. Methods in molecular biology™*, vol 452.

- Humana Press, Totowa: 331–363. [https://doi.org/10.1007/978-1-60327-159-2\\_16](https://doi.org/10.1007/978-1-60327-159-2_16).
- Jermiin, L. S., D. R. Lovell, B. Misof, P. G. Foster, & J. Robinson, 2020. Detecting and visualising the impact of heterogeneous evolutionary processes on phylogenetic estimates. *BioRxiv* 828996. <https://doi.org/10.1101/828996>.
- Jiao, X., T. Flouri, B. Rannala & Z. Yang, 2020. The impact of cross-species gene flow on species tree estimation. *Systematic Biology* 69: 830–847. <https://doi.org/10.1093/sysbio/syaa001>.
- Kalyaanamoorthy, S., B. Q. Minh, T. K. F. Wong, A. von Haeseler & L. S. Jermiin, 2017. ModelFinder: fast model selection for accurate phylogenetic estimates. *Nature Methods* 14: 587–589. <https://doi.org/10.1038/nmeth.4285>.
- Kapli, P., T. Flouri & M. J. Telford, 2021. Systematic errors in phylogenetic trees. *Current Biology* 31: R59–R64. <https://doi.org/10.1016/j.cub.2020.11.043>.
- Kapli, P., Z. Yang & M. J. Telford, 2020. Phylogenetic tree building in the genomic age. *Nature Reviews Genetics* 21: 428–444. <https://doi.org/10.1038/s41576-020-0233-0>.
- Kim, D. H., M. S. Kim, A. Hagiwara & J. S. Lee, 2021. The genome of the minute marine rotifer *Proales similis*: genome-wide identification of 401 G protein-coupled receptor (GPCR) genes. *Comparative Biochemistry and Physiology - Part D: Genomics and Proteomics* 39: 100861. <https://doi.org/10.1016/j.cbd.2021.100861>.
- Klopfstein, S., T. Massingham & N. Goldman, 2017. More on the best evolutionary rate for phylogenetic analysis. *Systematic Biology* 66: 769–785. <https://doi.org/10.1093/sysbio/syx051>.
- Kozlov, A. M., D. Darriba, T. Flouri, B. Morel & A. Stamatakis, 2019. RAxML-NG: a fast, scalable and user-friendly tool for maximum likelihood phylogenetic inference. *Bioinformatics* 35: 4453–4455. <https://doi.org/10.1093/bioinformatics/btz305>.
- Kristensen, R. M. & P. Funch, 2000. Micrognathozoa: a new class with complicated jaws like those of Rotifera and Gnathostomulida. *Journal of Morphology* 246: 1–49. [https://doi.org/10.1002/1097-4687\(200010\)246:1%3C1::AID-JMOR1%3E3.0.CO;2-D](https://doi.org/10.1002/1097-4687(200010)246:1%3C1::AID-JMOR1%3E3.0.CO;2-D).
- Kubatko, L. S. & J. H. Degnan, 2007. Inconsistency of phylogenetic estimates from concatenated data under coalescence. *Systematic Biology* 56: 17–24. <https://doi.org/10.1080/10635150601146041>.
- Kück, P., & Struck, T. H., 2014. BaCoCa - A heuristic software tool for the parallel assessment of sequence biases in hundreds of gene and taxon partitions. *Molecular Phylogenetics and Evolution*, 70, 94–98. <https://doi.org/10.1016/j.ympev.2013.09.011>.
- Kück, P., S. A. Meid, C. Groß, J. W. Wägele & B. Misof, 2014. AliGROOVE—visualization of heterogeneous sequence divergence within multiple sequence alignments and detection of inflated branch support. *BMC Bioinformatics* 15: 294. <https://doi.org/10.1186/1471-2105-15-294>.
- Kück, P., J. Romahn & K. Meusemann, 2022. Pitfalls of the site-concordance factor (sCF) as measure of phylogenetic branch support. *NAR Genomics and Bioinformatics* 4: lqac064. <https://doi.org/10.1093/nargab/lqac064>.
- Lanyon, S. M., 1988. The stochastic mode of molecular evolution: what consequences for systematic investigations? *The Auk* 105: 565–573. <https://doi.org/10.1093/auk/105.3.565>.
- Larose, C., G. Lavanchy, S. Freitas, D. J. Parker & T. Schwander, 2023. Facultative parthenogenesis: a transient state in transitions between sex and obligate asexuality in stick insects? *Peer Community Journal* 3: 60. <https://doi.org/10.24072/pcjournal.283>.
- Lartillot, N., 2020. PhyloBayes: Bayesian phylogenetics using site-heterogeneous models. In Scornavacca, C., F. Delsuc, & N. Galtier (eds), *Phylogenetics in the genomic era*. No commercial publisher | Authors open access book: 1.5:1–1.5:16. <https://hal.science/hal-02535342>.
- Lartillot, N., H. Brinkmann & H. Philippe, 2007. Suppression of long-branch attraction artefacts in the animal phylogeny using a site-heterogeneous model. *BMC Evolutionary Biology* 7: S4. <https://doi.org/10.1186/1471-2148-7-S1-S4>.
- Lartillot, N. & H. Philippe, 2004. A Bayesian mixture model for across-site heterogeneities in the amino-acid replacement process. *Molecular Biology and Evolution* 21: 1095–1109. <https://doi.org/10.1093/molbev/msh112>.
- Lartillot, N., N. Rodrigue, D. Stubbs & J. Richer, 2013. PhyloBayes MPI: phylogenetic reconstruction with infinite mixtures of profiles in a parallel environment. *Systematic Biology* 62: 611–615. <https://doi.org/10.1093/sysbio/syt022>.
- Lasek-Nesselquist, E., 2012. A mitogenomic re-evaluation of the bdelloid phylogeny and relationships among the Syndermata. *PLoS ONE* 7: e43554. <https://doi.org/10.1371/journal.pone.0043554>.
- Laumer, C. E., N. Bekkouche, A. Kerbl, F. Goetz, R. C. Neves, M. V. Sørensen, R. M. Kristensen, A. Hejnol, C. W. Dunn, G. Giribet & K. Worsaae, 2015. Spiralian phylogeny informs the evolution of microscopic lineages. *Current Biology* 25: 2000–2006. <https://doi.org/10.1016/j.cub.2015.06.068>.
- Laumer, C. E., R. Fernández, S. Lemer, D. Combosch, K. M. Kocot, A. Riesgo, S. C. S. Andrade, W. Sterrer, M. V. Sørensen & G. Giribet, 2019. Revisiting metazoan phylogeny with genomic sampling of all phyla. *Proceedings of the Royal Society B: Biological Sciences* 286: 20190831. <https://doi.org/10.1098/rspb.2019.0831>.
- Le, S. Q., O. Gascuel & N. Lartillot, 2008. Empirical profile mixture models for phylogenetic reconstruction. *Bioinformatics* 24: 2317–2323. <https://doi.org/10.1093/bioinformatics/btn445>.
- Lehmann, J., P. F. Stadler & V. Krauss, 2013. Near intron pairs and the metazoan tree. *Molecular Phylogenetics and Evolution* 66: 811–823. <https://doi.org/10.1016/j.ympev.2012.11.012>.
- Letunic, I. & P. Bork, 2021. Interactive tree of life (iTOL) v5: an online tool for phylogenetic tree display and annotation. *Nucleic Acids Research* 49: W293–W296. <https://doi.org/10.1093/nar/gkab301>.
- Li, C., K. A. Matthes-Rosana, M. Garcia & G. J. P. Naylor, 2012. Phylogenetics of Chondrichthyes and the problem of rooting phylogenies with distant outgroups. *Molecular*

- Phylogenetics and Evolution 63: 365–373. <https://doi.org/10.1016/j.ympcv.2012.01.013>.
- Lorenzen, S., 1985. Phylogenetic aspects of pseudocoelomate evolution. In Morris, S. C., J. D. George, R. Gibson & H. M. Platt (eds), *The Origins and Relationships of Lower Invertebrates*. Clarendon Press, Oxford.
- Maddison, W. P., 1997. Gene trees in species trees. *Systematic Biology* 46: 523–536. <https://doi.org/10.1093/sysbio/46.3.523>.
- Manni, M., Berkeley, M. R., Seppey, M., Simão, F. A., & Zdobnov, E. M., 2021. BUSCO update: novel and streamlined workflows along with broader and deeper phylogenetic coverage for scoring of eukaryotic, prokaryotic, and viral genomes. *Molecular Biology and Evolution*, 38, 4647–4654. <https://doi.org/10.1093/molbev/msab199>.
- Mark Welch, D. B., 2000. Evidence from a protein-coding gene that acanthocephalans are rotifers. *Invertebrate Biology* 119: 17–26. <https://doi.org/10.1111/j.1744-7410.2000.tb00170.x>.
- Mark Welch, D. B., 2005. Bayesian and maximum likelihood analyses of rotifer-acanthocephalan relationships. *Hydrobiologia* 546: 47–54. <https://doi.org/10.1007/s10750-005-4100-y>.
- Mark Welch, D. B., J. L. Mark Welch & M. Meselson, 2008. Evidence for degenerate tetraploidy in bdelloid rotifers. *Proceedings of the National Academy of Sciences* 105: 5145–5149. <https://doi.org/10.1073/pnas.0800972105>.
- Marlétaz, F., K. T. C. A. Peijnenburg, T. Goto, N. Satoh & D. S. Rokhsar, 2019. A new spiralian phylogeny places the enigmatic arrow worms among gnathiferans. *Current Biology* 29: 312–318. <https://doi.org/10.1016/j.cub.2018.11.042>.
- Mauer, K., S. L. Hellmann, M. Groth, A. C. Fröbuis, H. Zischler, T. Hankeln & H. Herlyn, 2020. The genome, transcriptome, and proteome of the fish parasite *Pomphorhynchus laevis* (Acanthocephala). *PLoS ONE* 15: e0232973. <https://doi.org/10.1371/journal.pone.0232973>.
- Mauer, K. M., H. Schmidt, M. Ditttrich, A. C. Fröbuis, S. L. Hellmann, H. Zischler, T. Hankeln & H. Herlyn, 2021. Genomics and transcriptomics of epizoic Seisonidea (Rotifera, syn. Syndermata) reveal strain formation and gradual gene loss with growing ties to the host. *BMC Genomics* 22: 604. <https://doi.org/10.1186/s12864-021-07857-y>.
- McCarthy, C. G. P., P. O. Mulhair, K. Siu-Ting, C. J. Creevey & M. J. O'Connell, 2023. Improving orthologous signal and model fit in datasets addressing the root of the animal phylogeny. *Molecular Biology and Evolution* 40: msac276. <https://doi.org/10.1093/molbev/msac276>.
- McKinney, W., 2010. Data structures for statistical computing in python. In van der Walt, S., & J. Millman (eds), *Proceedings of the 9th Python in Science Conference*: 51–56. <https://doi.org/10.25080/Majora-92bf1922-00a>.
- Melone, G., C. Ricci, H. Segers & R. L. Wallace, 1998. Phylogenetic relationships of phylum Rotifera with emphasis on the families of Bdelloidea. *Hydrobiologia* 387: 101–107. <https://doi.org/10.1023/A:1017057619574>.
- Mendes, F. K. & M. W. Hahn, 2018. Why concatenation fails near the anomaly zone. *Systematic Biology* 67: 158–169. <https://doi.org/10.1093/sysbio/syx063>.
- Min, G.-S. & J.-K. Park, 2009. Eurotatorian paraphyly: revisiting phylogenetic relationships based on the complete mitochondrial genome sequence of *Rotaria rotatoria* (Bdelloidea: Rotifera: Syndermata). *BMC Genomics* 10: 533. <https://doi.org/10.1186/1471-2164-10-533>.
- Minh, B. Q., M. W. Hahn & R. Lanfear, 2020a. New methods to calculate concordance factors for phylogenomic datasets. *Molecular Biology and Evolution* 37: 2727–2733. <https://doi.org/10.1093/molbev/msaa106>.
- Minh, B. Q., H. A. Schmidt, O. Chernomor, D. Schrempf, M. D. Woodhams, A. von Haeseler & R. Lanfear, 2020b. IQ-TREE 2: New models and efficient methods for phylogenetic inference in the genomic era. *Molecular Biology and Evolution* 37: 1530–1534. <https://doi.org/10.1093/molbev/msaa015>.
- Misof, B., B. Meyer, B. M. von Reumont, P. Kück, K. Misof & K. Meusemann, 2013. Selecting informative subsets of sparse supermatrices increases the chance to find correct trees. *BMC Bioinformatics* 14: 348. <https://doi.org/10.1186/1471-2105-14-348>.
- Mo, Y. K., R. Lanfear, M. W. Hahn & B. Q. Minh, 2023. Updated site concordance factors minimize effects of homoplasy and taxon sampling. *Bioinformatics* 39: btac741. <https://doi.org/10.1093/bioinformatics/btac741>.
- Mongiardino Koch, N., 2021. Phylogenomic subsampling and the search for phylogenetically reliable loci. *Molecular Biology and Evolution* 38: 4025–4038. <https://doi.org/10.1093/molbev/msab151>.
- Morel, B., A. M. Kozlov, A. Stamatakis & G. J. Szöllösi, 2020. GeneRax: a tool for species-tree-aware maximum likelihood-based gene family tree inference under gene duplication, transfer, and loss. *Molecular Biology and Evolution* 37: 2763–2774. <https://doi.org/10.1093/molbev/msaa141>.
- Morel, B., P. Schade, S. Lutteropp, T. A. Williams, G. J. Szöllösi & A. Stamatakis, 2022. SpeciesRax: a tool for maximum likelihood species tree inference from gene family trees under duplication, transfer, and loss. *Molecular Biology and Evolution* 39: msab365. <https://doi.org/10.1093/molbev/msab365>.
- Naser-Khdour, S., B. Q. Minh, W. Zhang, E. A. Stone, R. Lanfear & D. Bryant, 2019. The prevalence and impact of model violations in phylogenetic analysis. *Genome Biology and Evolution* 11: 3341–3352. <https://doi.org/10.1093/gbe/evz193>.
- Near, T. J., 2002. Acanthocephalan phylogeny and the evolution of parasitism. *Integrative and Comparative Biology* 42: 668–677. <https://doi.org/10.1093/icb/42.3.668>.
- Nguyen, L.-T., H. A. Schmidt, A. Von Haeseler & B. Q. Minh, 2015. IQ-TREE: a fast and effective stochastic algorithm for estimating maximum-likelihood phylogenies. *Molecular Biology and Evolution* 32: 268–274. <https://doi.org/10.1093/molbev/msu300>.
- Niehuis, O., G. Hartig, S. Grath, H. Pohl, J. Lehmann, H. Tafer, A. Donath, V. Krauss, C. Eisenhardt, J. Hertel, M. Petersen, C. Mayer, K. Meusemann, R. S. Peters, P. F. Stadler, R. G. Beutel, E. Bornberg-Bauer, D. D. McKenna & B. Misof, 2012. Genomic and morphological evidence converge to resolve the enigma of Strepsiptera. *Current Biology* 22: 1309–1313. <https://doi.org/10.1016/j.cub.2012.05.018>.

- Nowell, R. W., P. Almeida, C. G. Wilson, T. P. Smith, D. Fontaneto, A. Crisp, G. Micklem, A. Tunnacliffe, C. Boschetti & T. G. Barraclough, 2018. Comparative genomics of bdelloid rotifers: insights from desiccating and non-desiccating species. *PLoS Biology* 16: e2004830. <https://doi.org/10.1371/journal.pbio.2004830>.
- Nowell, R. W., C. G. Wilson, P. Almeida, P. H. Schiffer, D. Fontaneto, L. Becks, F. Rodriguez, I. R. Arkhipova & T. G. Barraclough, 2021. Evolutionary dynamics of transposable elements in bdelloid rotifers. *eLife* 10: e63194. <https://doi.org/10.7554/eLife.63194>.
- Ontano, A. Z., G. Gainett, S. Aharon, J. A. Ballesteros, L. R. Benavides, K. F. Corbett, E. Gavish-Regev, M. S. Harvey, S. Monsma, C. E. Santibáñez-López, E. V. W. Setton, J. T. Zehms, J. A. Zeh, D. W. Zeh & P. P. Sharma, 2021. Taxonomic sampling and rare genomic changes overcome long-branch attraction in the phylogenetic placement of Pseudoscorpions. *Molecular Biology and Evolution* 38: 2446–2467. <https://doi.org/10.1093/molbev/msab038>.
- Parey, E., A. Louis, J. Montfort, O. Bouchez, C. Roques, C. Iampietro, J. Lluch, A. Castinel, C. Donnadiou, T. Desvignes, C. F. Bucaco, E. Jouanno, M. Wen, S. Mejri, R. P. Dirks, H. J. Jansen, C. V. Henkel, W.-J. Chen, M. Zahm, C. Cabau, C. Klopp, A. W. Thompson, M. Robinson-Rechavi, I. Braasch, G. Lecointre, J. Bobe, J. H. Postlethwait, C. Berthelot, H. Roest Crolius & Y. Guiguen, 2023. Genome structures resolve the early diversification of teleost fishes. *Science* 379: 572–575. <https://doi.org/10.1126/science.abq4257>.
- Philippe, H., H. Brinkmann, D. V. Lavrov, D. T. J. Littlewood, M. Manuel, G. Wörheide & D. Baurain, 2011. Resolving difficult phylogenetic questions: why more sequences are not enough. *PLoS Biology* 9: e1000602. <https://doi.org/10.1371/journal.pbio.1000602>.
- Philippe, H., R. Derelle, P. Lopez, K. Pick, C. Borchellini, N. Boury-Esnault, J. Vacelet, E. Renard, E. Houlston, E. Quéinnec, C. Da Silva, P. Wincker, H. Le Guyader, S. Leys, D. J. Jackson, F. Schreiber, D. Erpenbeck, B. Morgenstern, G. Wörheide & M. Manuel, 2009. Phylogenomics revives traditional views on deep animal relationships. *Current Biology* 19: 706–712. <https://doi.org/10.1016/j.cub.2009.02.052>.
- Philippe, H. & J. Laurent, 1998. How good are deep phylogenetic trees? *Current Opinion in Genetics & Development* 8: 616–623. [https://doi.org/10.1016/S0959-437X\(98\)80028-2](https://doi.org/10.1016/S0959-437X(98)80028-2).
- Philippe, H. & B. Roure, 2011. Difficult phylogenetic questions: more data, maybe; better methods, certainly. *BMC Biology* 9: 91. <https://doi.org/10.1186/1741-7007-9-91>.
- Phillips, M. J. & D. Penny, 2003. The root of the mammalian tree inferred from whole mitochondrial genomes. *Molecular Phylogenetics and Evolution* 28: 171–185. [https://doi.org/10.1016/S1055-7903\(03\)00057-5](https://doi.org/10.1016/S1055-7903(03)00057-5).
- Pisani, D., M. J. Benton & M. Wilkinson, 2007. Congruence of morphological and molecular phylogenies. *Acta Biotheoretica* 55: 269–281. <https://doi.org/10.1007/s10441-007-9015-8>.
- Pisani, D., W. Pett, M. Dohrmann, R. Feuda, O. Rota-Stabelli, H. Philippe, N. Lartillot & G. Wörheide, 2015. Genomic data do not support comb jellies as the sister group to all other animals. *Proceedings of the National Academy of Sciences* 112: 15402–15407. <https://doi.org/10.1073/pnas.1518127112>.
- R Core Team, 2021. R: a language and environment for statistical computing. Vienna, Austria, <https://www.r-project.org/>.
- Ragsdale, E. J. & J. G. Baldwin, 2010. Resolving phylogenetic incongruence to articulate homology and phenotypic evolution: a case study from Nematoda. *Proceedings of the Royal Society b: Biological Sciences* 277: 1299–1307. <https://doi.org/10.1098/rspb.2009.2195>.
- Ricci, C., 1998. Are lemnisci and proboscis present in the Bdelloidea? *Hydrobiologia* 387: 93–96. <https://doi.org/10.1023/A:1017091104243>.
- Ricci, C., G. Melone & C. Sotgia, 1993. Old and new data on Seisonidea (Rotifera). *Hydrobiologia* 255: 495–511. <https://doi.org/10.1007/BF00025879>.
- Roch, S., M. Nute & T. Warnow, 2019. Long-branch attraction in species tree estimation: inconsistency of partitioned likelihood and topology-based summary methods. *Systematic Biology* 68: 281–297. <https://doi.org/10.1093/sysbio/syy061>.
- Roch, S. & T. Warnow, 2015. On the robustness to gene tree estimation error (or lack thereof) of coalescent-based species tree methods. *Systematic Biology* 64: 663–676. <https://doi.org/10.1093/sysbio/syv016>.
- Rozanski, A., H. Moon, H. Brandl, J. M. Martín-Durán, M. A. Grohme, K. Hüttner, K. Bartscherer, I. Henry & J. C. Rink, 2019. PlanMine 3.0—improvements to a mineable resource of flatworm biology and biodiversity. *Nucleic Acids Research* 47: D812–D820. <https://doi.org/10.1093/nar/gky1070>.
- Salichos, L. & A. Rokas, 2013. Inferring ancient divergences requires genes with strong phylogenetic signals. *Nature* 497: 327–331. <https://doi.org/10.1038/nature12130>.
- Schultz, D. T., S. H. D. Haddock, J. V. Bredeson, R. E. Green, O. Simakov & D. S. Rokhsar, 2023. Ancient gene linkages support ctenophores as sister to other animals. *Nature* 618: 110–117. <https://doi.org/10.1038/s41586-023-05936-6>.
- Segers, H. & G. Melone, 1998. A comparative study of trophi morphology in Seisonidea (Rotifera). *Journal of Zoology* 244: 201–207. <https://doi.org/10.1111/j.1469-7998.1998.tb00025.x>.
- Sharma, P. P., J. A. Ballesteros & C. E. Santibáñez-López, 2021. What is an “arachnid”? Consensus, consilience, and confirmation bias in the phylogenetics of Chelicerata. *Diversity* 13: 568. <https://doi.org/10.3390/d13110568>.
- Sielaff, M., H. Schmidt, T. H. Struck, D. Rosenkranz, D. B. Mark Welch, T. Hankeln & H. Herlyn, 2016. Phylogeny of Syndermata (syn. Rotifera): mitochondrial gene order verifies epizoic Seisonidea as sister to endoparasitic Acanthocephala within monophyletic Hemirofifera. *Molecular Phylogenetics and Evolution* 96: 79–92. <https://doi.org/10.1016/j.ympev.2015.11.017>.
- Simakov, O., J. Bredeson, K. Berkoff, F. Marletaz, T. Mitros, D. T. Schultz, B. L. O’Connell, P. Dear, D. E. Martinez, R. E. Steele, R. E. Green, C. N. David & D. S. Rokhsar, 2022. Deeply conserved synteny and the evolution



- of metazoan chromosomes. *Science Advances* 8: 5884. <https://doi.org/10.1126/sciadv.abi5884>.
- Simion, P., F. Delsuc, & H. Philippe, 2020. To what extent current limits of phylogenomics can be overcome? In Scornavacca, C., F. Delsuc, & N. Galtier (eds), *Phylogenetics in the genomic era*. No commercial publisher | Authors' open access book: 2.1:1–2.1:34. <https://hal.archives-ouvertes.fr/hal-02535366>.
- Simion, P., J. Narayan, A. Houtain, A. Derzelle, L. Baudry, E. Nicolas, R. Arora, M. Cariou, C. Cruaud, F. R. Gaudray, C. Gilbert, N. Guiglielmoni, B. Hespels, D. K. L. Kozłowski, K. Labadie, A. Limasset, M. Llirós, M. Marbouty, M. Terwagne, J. Virgo, R. Cordaux, E. G. J. Danchin, B. Hallet, R. Koszul, T. Lenormand, J. F. Flot & K. Van Doninck, 2021. Chromosome-level genome assembly reveals homologous chromosomes and recombination in asexual rotifer *Adineta vaga*. *Science Advances* 7: eabg4216. <https://doi.org/10.1126/sciadv.abg4216>.
- Siu-Ting, K., M. Torres-Sánchez, D. San Mauro, D. Wilcockson, M. Wilkinson, D. Pisani, M. J. O'Connell & C. J. Creevey, 2019. Inadvertent paralog inclusion drives artifactual topologies and timetree estimates in phylogenomics. *Molecular Biology and Evolution* 36: 1344–1356. <https://doi.org/10.1093/molbev/msz067>.
- Smith, M. L. & M. W. Hahn, 2021. New approaches for inferring phylogenies in the presence of paralogs. *Trends in Genetics* 37: 174–187. <https://doi.org/10.1016/j.tig.2020.08.012>.
- Sørensen, M. V., R. M. Kristensen & K. Worsaae, 2016. The Gnathifera. Phyla Gnathostomulida, Rotifera (including Acanthocephala), and Micrognathozoa. In Brusca, R. C., W. Moore & S. M. Shuster (eds), *Invertebrates* Sinauer Associates, Sunderland: 613–634.
- Sørensen, M. V. & R. M. Kristensen, 2015. Micrognathozoa. In Schmidt-Rhaesa, A. (ed), *Handbook of zoology*, Vol. 3. De Gruyter, Berlin: 197–216. *Gastrotricha and Gnathifera*.
- Sørensen, M. V., 2002. On the evolution and morphology of the rotiferan trophi, with a cladistic analysis of Rotifera. *Journal of Zoological Systematics and Evolutionary Research* 40: 129–154. <https://doi.org/10.1046/j.1439-0469.2002.00188.x>.
- Sørensen, M. V., 2003. Further structures in the jaw apparatus of *Limnognathia maerski* (Micrognathozoa), with notes on the phylogeny of the Gnathifera. *Journal of Morphology* 255: 131–145. <https://doi.org/10.1002/jmor.10038>.
- Sørensen, M. V., P. Funch, E. Willerslev, A. J. Hansen & J. Olesen, 2000. On the phylogeny of the Metazoa in the light of Cyclophora and Micrognathozoa. *Zoologischer Anzeiger* 239: 297–318.
- Sørensen, M. V. & G. Giribet, 2006. A modern approach to rotiferan phylogeny: combining morphological and molecular data. *Molecular Phylogenetics and Evolution* 40: 585–608. <https://doi.org/10.1016/j.ympev.2006.04.001>.
- Springer, M. S. & J. Gatesy, 2016. The gene tree delusion. *Molecular Phylogenetics and Evolution* 94: 1–33. <https://doi.org/10.1016/j.ympev.2015.07.018>.
- Stamatakis, A., & A. M. Kozlov, 2020. Efficient maximum likelihood tree building methods. In Scornavacca, C., F. Delsuc, & N. Galtier (eds), *Phylogenetics in the genomic era*. No commercial publisher | Authors open access book: 1.2 :1–1.2:18. <https://hal.science/hal-02535285v2>.
- Steenwyk, J. L., T. J. Buida III., A. L. Labella, Y. Li, X.-X. Shen & A. Rokas, 2021. PhyKIT: a broadly applicable UNIX shell toolkit for processing and analyzing phylogenomic data. *Bioinformatics* 37: 2325–2331. <https://doi.org/10.1093/bioinformatics/btab096>.
- Steenwyk, J. L., D. C. Goltz, T. J. Buida III., Y. Li, X.-X. Shen & A. Rokas, 2022. OrthoSNAP: a tree splitting and pruning algorithm for retrieving single-copy orthologs from gene family trees. *PLOS Biology* 20: e3001827. <https://doi.org/10.1371/journal.pbio.3001827>.
- Sterrer, W., 1972. Systematics and evolution within the Gnathostomulida. *Systematic Zoology* 21: 151–173. <https://doi.org/10.2307/2412286>.
- Storch, V. & U. Welsch, 1969. Über den Aufbau des Rotatorienintegumentes. *Zeitschrift für Zellforschung und Mikroskopische Anatomie* 95: 405–414. <https://doi.org/10.1007/BF00995213>.
- Struck, T. H., 2014. TreSpEx-Detection of misleading signal in phylogenetic reconstructions based on tree information. *Evolutionary Bioinformatics* 10: 51–67. <https://doi.org/10.4137/EBO.S14239>.
- Struck, T. H., A. R. Wey-Fabrizius, A. Golombek, L. Hering, A. Weigert, C. Bleidorn, S. Klebow, N. Iakovenko, B. Hausdorf, M. Petersen, P. Kück, H. Herlyn & T. Hankeln, 2014. Platyzoan paraphyly based on phylogenomic data supports a noncoelomate ancestry of Spiralia. *Molecular Biology and Evolution* 31: 1833–1849. <https://doi.org/10.1093/molbev/msu143>.
- Terwagne, M., E. Nicolas, B. Hespels, L. Herter, J. Virgo, C. Demazy, A. C. Heuskin, B. Hallet & K. Van Doninck, 2022. DNA repair during nonreductional meiosis in the asexual rotifer *Adineta vaga*. *Science Advances* 8: eadc8829. <https://doi.org/10.1126/sciadv.adc8829>.
- Tihelka, E., C. Cai, M. Giacomelli, J. Lozano-Fernandez, O. Rota-Stabelli, D. Huang, M. S. Engel, P. C. J. Donoghue & D. Pisani, 2021. The evolution of insect biodiversity. *Current Biology* 31: R1299–R1311. <https://doi.org/10.1016/j.cub.2021.08.057>.
- Vasilikopoulos, A., M. Balke, R. G. Beutel, A. Donath, L. Podsiadłowski, J. M. Pflug, R. M. Waterhouse, K. Meusemann, R. S. Peters, H. E. Escalona, C. Mayer, S. Liu, L. Hendrich, Y. Alarie, D. T. Bilton, F. Jia, X. Zhou, D. R. Maddison, O. Niehuis & B. Misof, 2019. Phylogenomics of the superfamily Dytiscoidea (Coleoptera: Adephaga) with an evaluation of phylogenetic conflict and systematic error. *Molecular Phylogenetics and Evolution* 135: 270–285. <https://doi.org/10.1016/j.ympev.2019.02.022>.
- Vasilikopoulos, A., M. Balke, S. Kukowka, J. M. Pflug, S. Martin, K. Meusemann, L. Hendrich, C. Mayer, D. R. Maddison, O. Niehuis, R. G. Beutel & B. Misof, 2021a. Phylogenomic analyses clarify the pattern of evolution of Adephaga (Coleoptera) and highlight phylogenetic artefacts due to model misspecification and excessive data trimming. *Systematic Entomology* 46: 991–1018. <https://doi.org/10.1111/syen.12508>.

- Vasilikopoulos, A., G. T. Gustafson, M. Balke, O. Niehuis, R. G. Beutel & B. Misof, 2021. Resolving the phylogenetic position of Hygrobiidae (Coleoptera: Adephaga) requires objective statistical tests and exhaustive phylogenetic methodology: a response to Cai et al (2020). *Molecular Phylogenetics and Evolution* 162: 106923. <https://doi.org/10.1016/j.ympev.2020.106923>.
- von Haffner, K., 1950. Organisation und systematische Stellung der Acanthocephalen. *Zoologischer Anzeiger* 145: 243–274.
- Wallace, R. L., 2002. Rotifers: exquisite metazoans. *Integrative and Comparative Biology* 42: 660–667. <https://doi.org/10.1093/icb/42.3.660>.
- Wallace, R. L., & R. A. Colburn, 1989. Phylogenetic relationships within phylum Rotifera: orders and genus *Notholca*. In Ricci, C., T. W. Snell, & C. E. King (eds), *Rotifer Symposium V. Developments in Hydrobiology*, vol 52. Springer, Dordrecht: 311–318. [https://doi.org/10.1007/978-94-009-0465-1\\_37](https://doi.org/10.1007/978-94-009-0465-1_37).
- Wallace, R. L., C. Ricci & G. Melone, 1996. A cladistic analysis of pseudocoelomate (aschelminth) morphology. *Invertebrate Biology* 115: 104–112. <https://doi.org/10.2307/3227041>.
- Wang, Y., H. Tang, J. D. Debarry, X. Tan, J. Li, X. Wang, T. H. Lee, H. Jin, B. Marler, H. Guo, J. C. Kissinger & A. H. Paterson, 2012. MScanX: a toolkit for detection and evolutionary analysis of gene synteny and collinearity. *Nucleic Acids Research* 40: e49. <https://doi.org/10.1093/nar/gkr1293>.
- Waskom, M. L., 2021. Seaborn: statistical data visualization. *Journal of Open Source Software* 6: 3021. <https://doi.org/10.21105/joss.03021>.
- Wey-Fabrizius, A. R., H. Herlyn, B. Rieger, D. Rosenkranz, A. Witek, D. B. Mark Welch, I. Ebersberger & T. Hankeln, 2014. Transcriptome data reveal syndermatan relationships and suggest the evolution of endoparasitism in Acanthocephala via an epizoic stage. *PLoS ONE* 9: e88618. <https://doi.org/10.1371/journal.pone.0088618>.
- Whelan, S., I. Irisarri & F. Burki, 2018. PREQUAL: detecting non-homologous characters in sets of unaligned homologous sequences. *Bioinformatics* 34: 3929–3930. <https://doi.org/10.1093/bioinformatics/bty448>.
- Winnepenninckx, B., T. Backeljau, L. Y. Mackey, J. M. Brooks, R. De Wachter, S. Kumar & J. R. Garey, 1995. 18S rRNA data indicate that Aschelminthes are polyphyletic in origin and consist of at least three distinct clades. *Molecular Biology and Evolution* 12: 1132–1137. <https://doi.org/10.1093/oxfordjournals.molbev.a040287>.
- Winnepenninckx, B. M. H., T. Backeljau & R. M. Kristensen, 1998. Relations of the new phylum Cyclophora. *Nature* 393: 636–638. <https://doi.org/10.1038/31377>.
- Witek, A., H. Herlyn, I. Ebersberger, D. B. Mark Welch & T. Hankeln, 2009. Support for the monophyletic origin of Gnathifera from phylogenomics. *Molecular Phylogenetics and Evolution* 53: 1037–1041. <https://doi.org/10.1016/j.ympev.2009.07.031>.
- Witek, A., H. Herlyn, A. Meyer, L. Boell, G. Bucher & T. Hankeln, 2008. EST based phylogenomics of Syndermata questions monophyly of Eurotatoria. *BMC Evolutionary Biology* 8: 345. <https://doi.org/10.1186/1471-2148-8-345>.
- Wong, T. K. F., Kalyaanamoorthy, S., Meusemann, K., Yeates, D. K., Misof, B., & Jermini, L. S., 2020. A minimum reporting standard for multiple sequence alignments. *NAR Genomics and Bioinformatics*, 2, lqaa024. <https://doi.org/10.1093/nargab/lqaa024>.
- Zhang, C. & S. Mirarab, 2022. ASTRAL-Pro 2: ultrafast species tree reconstruction from multi-copy gene family trees. *Bioinformatics* 38: 4949–4950. <https://doi.org/10.1093/bioinformatics/btac620>.
- Zhang, C., C. Scornavacca, E. K. Molloy & S. Mirarab, 2020. ASTRAL-Pro: quartet-based species-tree inference despite paralogy. *Molecular Biology and Evolution* 37: 3292–3307. <https://doi.org/10.1093/molbev/msaa139>.
- Zhao, T., A. Zwaenepoel, J.-Y. Xue, S.-M. Kao, Z. Li, M. E. Schranz & Y. Van de Peer, 2021. Whole-genome microsynteny-based phylogeny of angiosperms. *Nature Communications* 12: 3498. <https://doi.org/10.1038/s41467-021-23665-0>.
- Zhong, M., Hansen, B., Nesnidal, M., Golombek, A., Halanych, K. M., & Struck, T. H., 2011. Detecting the symplesiomorphy trap: a multigene phylogenetic analysis of terebelliform annelids. *BMC Evolutionary Biology*, 11, 369. <https://doi.org/10.1186/1471-2148-11-369>.
- Zrzavý, J., 2001. The interrelationships of metazoan parasites: a review of phylum- and higher-level hypotheses from recent morphological and molecular phylogenetic analyses. *Folia Parasitologica* 48: 81–103. <https://doi.org/10.14411/fp.2001.013>.

**Publisher's Note** Springer Nature remains neutral with regard to jurisdictional claims in published maps and institutional affiliations.

Springer Nature or its licensor (e.g. a society or other partner) holds exclusive rights to this article under a publishing agreement with the author(s) or other rightsholder(s); author self-archiving of the accepted manuscript version of this article is solely governed by the terms of such publishing agreement and applicable law.